

Dear Editor,

Please find hereinafter a point-by-point response to the review of both Referees, as well as a track changes version of the manuscript. We took each point into consideration and revised our manuscript accordingly.

We hope that the revised version will reach the quality standard of ACP.

On behalf of all co-authors,

Best regards,

Jean-Eudes Petit

#### Anonymous Referee #1h

The authors thank Referee #1 for highlighting the originality of the present article.

The reporting of response factors is indeed essential for ACSM measurements.

In this respect, a dedicated table and a small paragraph will be added in the revised manuscript:

“Throughout the measuring period, three Response Factor (RF) calibrations and one  $(\text{NH}_4)_2\text{SO}_4$  calibrations were performed, summarized in Table 1. The low drift of the obtained slopes allowed the use of an average response factor of  $2.72 \cdot 10^{-11}$  (with an standard deviation of  $\pm 13\%$ ).”

Table 1. Response factors obtained through IE calibrations from June 2011 to May 2013

Date	Response Factor	$\text{RIE}_{\text{NH}_4}$	$\text{RIE}_{\text{SO}_4}$
16/11/2011	$2.31 \cdot 10^{-11}$	6	-
09/10/2012	$2.98 \cdot 10^{-11}$	4.8	-
15/05/2013	$2.84 \cdot 10^{-11}$	6.84	1.25
<b>Average</b>	<b><math>2.72 \cdot 10^{-11}</math></b>	<b>5.88</b>	-
<b>Standard deviation</b>	<b>13%</b>	<b>17%</b>	-

#### Anonymous Referee #2

The authors thank Referee #2 for all comments that have been raised.

The thorough evaluation of such novel instrumentation is much needed. A European intercomparison exercise has been carried out at SIRTa in November 2013, involving 13 ACSMs, and represents a unique opportunity to assess the reproducibility of ACSM instruments (Crenn et al., in preparation). Some lines will be added on this subject:

“A comprehensive determination of the overall uncertainty (as well as  $\text{PM}_{10}$  components) associated to ACSM-derived measurements has been carried out in November 2013 through an inter-comparison exercise (Crenn et al., in preparation; Fröhlich et al., 2015). Here, the consistency of ACSM measurements has been assessed from the comparison with co-located measurements, as described in Section 3.”

With the presented dataset, we chose to compare the ACSM with collocated instruments at different timescales (high/low temporal resolution) over different temporal windows (short-/long-term). In this context, we only used  $\text{PM}_{10}$  TEOM-FDMS data,  $\text{PM}_{10}$  PILS-IC data and  $\text{PM}_{2.5}$  filters.

The source apportionment of the organic fraction over long-term periods is scientifically very interesting, and although this topic is not covered in this article, it will be emphasized in the conclusion as a perspective:

“In parallel, the long-term characterization of the organic fraction would surely lead to a better assessment of aerosol sources and some (trans-)formation processes of secondary pollution in the Ile-de-France area.”

Please also note that a dedicated paragraph on this subject is already present in section 2.4.

### Specific comments

*1. Page 24227, line 21. ACSM measures PM1 aerosols (unless they have a PM2.5 lens). Do the authors mean that they used a PM2.5 cyclone at the inlet?*

**AR:** Yes, we used a PM2.5 cyclone inlet (in order to prevent coarse particles from reaching the PM1 aerodynamic lens of the ACSM). It will be clearly stated in the manuscript as follows:

“Briefly, PM<sub>2.5</sub> aerosols are sampled at 3 L/min (from a PM<sub>2.5</sub> cyclone inlet) and then sub-sampled at 85 mL/min (volumetric flow) through an aerodynamic lens”

*2. Page 24228, line 6. Technically, for ACSM, it should be “response factor” (see Ng et al), not “ionization efficiency”. Also, what is the variation in the response factor throughout the whole campaign? How often as calibration performed? What is the data saving interval? (every 30mins?)*

**AR:** Yes, we agree. As also mentioned by Referee#1, more information should be given on this RF calibration. In this respect, a dedicated table and a small paragraph will be added in the revised manuscript (please see above our response to Referee#1)

The temporal resolution is indeed about 30 min, which will be specified in the manuscript as follows:

“A total number of ~26,000 ACSM data points (with a temporal resolution of 30 min) were collected from June 2011 to June 2013”

*3. Page 24230, line 21. Are these TEOM data?*

**AR:** Yes. It will be clearly stated in the manuscript:

“Hourly PM<sub>2.5</sub> data from TEOM-FDMS measurements were retrieved from the three stations representative of the Paris urban background”

*4. Page 24233, nitrate discussion. It is not clear how “no overestimation of ACSM nitrate is observed at high concentrations” would suggest “the ability of the Middlebrook algorithm to properly correct our ACSM collection efficiencies”. If “proper” CE means that concentration of the species measured by the ACSM is in agreement with other measurements, then all other species (sulfate, etc) should also be in agreement with other measurements? (but this is not quite the case).*

**AR:** The collection efficiency is influenced by the mass fraction of ammonium nitrate (Middlebrook et al., 2012). To assess the validity of this correction, we used PM1 PILS-IC measurements. The quasi perfect match between the 2 instruments (slope of 0.99) underlines the “ability of the Middlebrook algorithm to properly correct our ACSM collection efficiencies”. Then, although filters measurements can be influenced by some sampling artefacts and that sampling was performed at PM<sub>2.5</sub>, the good slope (0.91) and  $r^2$  lead to the same conclusion.

A different behavior is observed for sulphate, as it may be influenced by other types of artifacts that are not fully understood yet (Crenn et al., in prep; Frohlich et al., 2015). It is also to note that the determination of sulphate concentrations is furthermore subject to the determination of a specific Relative Ion Efficiency, independently of the choice of adequate CEs.

*5. Page 24233-24234. It is not clear why the authors compared the PM1 ACSM data to PM2.5 filter data. It appears that PM1 filter data are available (see Figure 3). They should compare ACSM data to PM1 filter data.*

**AR:** Figure 3 refers to the comparison with PM1 TEOM-FDMS. Unfortunately, there was no PM1 filter measurement available. This will be more clearly specified in the revised manuscript.

Nevertheless, we would like to underline that previous AMS (PM1) and PILS-IC (PM2.5) measurements in the region of Paris have shown very similar results, emphasizing on the fact that the fraction between 1 and 2.5  $\mu\text{m}$  is not significant in this region (Freutel et al., 2013; Crippa et al., 2013).

*6. Page 24233, sulfate comparison. Can the authors compare their PM1 sulfate data and PM2.5 sulfate data to support their hypothesis that sulfate associated with larger particles is a cause for the difference between ACSM and filter sulfate comparison?*

**AR:** Unfortunately, there was no PM1 filter measurement available, and no PM1 vs. PM2.5 sulphate data obtained from the same methodology could be done. Moreover, various reasons can be raised to explain the observed discrepancies between PM1 SO<sub>4</sub> from ACSM measurements and PM2.5 SO<sub>4</sub> from filter sampling, such as size distribution and artifacts peculiar to the sampling technique. All combined, they might lead to compensatory errors, making it difficult to thoroughly determine the contribution of each artifact.

*7. Page 24233, line 26. Is it appropriate to compare ACSM OM to PM2.5 OC? Please justify this.*

**AR:** The comparison of ACSM OM with PM2.5 OC does not lead to a thorough conversion factor, although it has been shown that i) a few percentage of OM is located between 1 and 2.5  $\mu\text{m}$  (Favez et al., 2007); and ii) the use of a constant OC-to-OM conversion factor is reasonable throughout the year as it brings to very satisfactory PM mass closure (Bressi et al., 2013). However, the relatively good  $r^2$  obtained after the regression indicates that the temporal variations of ACSM OM make sense; but it does not directly validate absolute concentrations.

*8. Page 24235, line 9. What discrepancies?*

**AR:** These discrepancies are linked to an interannual variability observed in Fig. S2. The following sentences will be added for clarity: “The highest observed discrepancies occur with highest measured mass, which may highlight an intensification of pollution episodes. On a broader perspective, this feature is also observed through inter-annual variability of urban background PM<sub>2.5</sub> concentrations (Fig. S2).”

*9. Page 24236, lines 16. Why such a feature is only observed here but not in previous measurements (Megapoli/Ariparif-Particules projects)?*

**AR:** This feature has not been seen during PARTICULES, essentially due to a low time resolution (daily filter sampling), and has not been investigated during MEGAPOLI. It will be clearly stated in the manuscript:

“, a feature which has not been seen during the AIRPARIF-Particules projects, essentially due to highly time resolved measurements, nor investigated during the MEGAPOLI project”

*10. Page 24241, line 4. This citation is for isoprene SOA. Do the authors expect high contributions of isoprene SOA in the region?*

**AR:** The determination from on-site measurements of the contribution of biogenic SOA in urban environments can be challenging, because isoprene can be emitted in significant amounts by anthropogenic sources. Von Schneidemesser et al. (2011) and Crippa et al. (2013) estimated a low contribution of isoprene on the OH reactivity in Paris. Modelling studies show conversely a much higher contribution (more than 90%) of biogenic SOA in Paris, especially in summer (Petetin et al., 2014).

*11. Page 24241, line 5. It seems that nitrate and OM have a more different diurnal trends on the weekends. Why?*

**AR:** Nitrate and OM show indeed a slightly different pattern during the week-end, in winter and summer, respectively. However, the scales are quite zoomed in, and as we do not want to overinterpret the data, we decided to focus on more obvious general trends.

*12. Figure 6. Please states clearly how seasons are defined (which month to which month). I suggest using a different color scheme for the seasons, so as not to be confused with ACSM species. It is not clear what the authors meant by “each data point correspond to 1 ACSM measurement”.*

**AR:** Seasons were differentiated by the seasonal equinoxes. This will be clearly stated in the manuscript.

By “each data point correspond to 1 ACSM measurement”, we wanted to emphasize on the fact that each average bin has been calculated from 30-min ACSM datapoint. As this may add some confusion; the sentence will be deleted.

**13.** *Figure 7. What is SO<sub>4</sub><sup>2-</sup> in this figure? Sulfate measured by ACSM? PM<sub>1</sub> filter sulfate? PM<sub>2.5</sub> filter sulfate?*

**AR:** It corresponds to ACSM (PM<sub>1</sub>) SO<sub>4</sub><sup>2-</sup>. It will be clearly stated in the figure caption.

**14.** *Figure 8, what is the color scale of the wind rose? Why NH<sub>4</sub> data are not included in this figure?*

**AR:** The color scale represents the Joint Probability Function (described in Henry et al., 2009), and corresponds somewhat to the occurrence of any wind direction and speed. A colorbar will be added for clarity.

NH<sub>4</sub> is not included in the NWR because, as it is quasi entirely combined to NO<sub>3</sub> and SO<sub>4</sub>, it would lead to redundant information.

**15.** *Figure 10, why is sulfate data not included here?*

**AR:** Sulphate presents poor diurnal variations (average of 0.75 µg/m<sup>3</sup> ± 2%), linked with the fact that sulphate is mostly advected over the Ile-de-France region, and de facto not influenced by potential local sources. This is why we didn't include this specie. More precision will be added: "Sulphate variations are not presented and discussed here because they lead to poor daily variations (average of 0.75 µg/m<sup>3</sup> ± 2%), which are consistent with its mid-to-long range transport origin"

**16.** *I think the authors intended to use BC / SO<sub>4</sub> to denote local vs. regional/advected pollution. However, throughout the manuscript, there are multiple sentences noting that this ratio is used to denote local/regional vs. advected PM – this needs to be corrected.*

**AR:** The use of the BC/SO<sub>4</sub> ratio was intended to assess local, regional, and advected patterns. However, this distinction was, indeed, not evident throughout the manuscript. It will be corrected throughout the manuscript, as follows:

"BC-to-sulphate ratio used here as a proxy of the local / regional / advected contribution of PM"

## References

Bressi, M., Sciare, J., Gherzi, V., Bonnaire, N., Nicolas, J. B., Petit, J.-E., Moukhtar, S., Rosso, A., Mihalopoulos, N. and Féron, A.: A one-year comprehensive chemical characterisation of fine aerosol (PM<sub>2.5</sub>) at urban, suburban and rural background sites in the region of Paris (France), *Atmospheric Chem. Phys.*, 13(15), 7825–7844, doi:10.5194/acp-13-7825-2013, 2013.

Crenn, V., Frohlich, R., Sciare, J., Croteau, P., Favez, O., Verlhac, S., Belis, C.A., Aas, W.,

Aijala, M., Artinano, B., Baisnée, D., Baltensperger, U., Bonnaire, N., Bressi, M., Canagaratna, M., Canonaco, F., Carbone, C., Cavalli, F., Coz, E., Cubison, M.J., Gietl, J., Green, D., Gros, V., Heikkinen, L., Lunder, C., Minguillon, M., Mocnik, G., O'Down, C., Ovadnevaite, J., Petit, J.-E., Petralia, E., Poulain, L., Prevot, A.S.H., Priestman, M., Riffault, V., Ripoli, A., Sarda-Estève, R., Slowik, J.G., Setyan, A., Jayne, J.: Results of the ACTRIS ACSM intercomparison at the SIRTa French atmospheric supersite in the region of Paris, in preparation.

Bressi, M., Sciare, J., Gherzi, V., Bonnaire, N., Nicolas, J. B., Petit, J.-E., Moukhtar, S., Rosso, A., Mihalopoulos, N. and Féron, A.: A one-year comprehensive chemical characterisation of fine aerosol (PM<sub>2.5</sub>) at urban, suburban and rural background sites in the region of Paris (France), *Atmospheric Chem. Phys.*, 13(15), 7825–7844, doi:10.5194/acp-13-7825-2013, 2013.

Crippa, M., DeCarlo, P. F., Slowik, J. G., Mohr, C., Heringa, M. F., Chirico, R., Poulain, L., Freutel, F., Sciare, J., Cozic, J., Di Marco, C. F., Elsasser, M., Nicolas, J. B., Marchand, N., Abidi, E., Wiedensohler, A., Drewnick, F., Schneider, J., Borrmann, S., Nemitz, E., Zimmermann, R., Jaffrezo, J.-L., Prévôt, A. S. H. and Baltensperger, U.: Wintertime aerosol chemical composition and source apportionment of the organic fraction in the metropolitan area of Paris, *Atmospheric Chem. Phys.*, 13(2), 961–981, doi:10.5194/acp-13-961-2013, 2013.

Favez, O., Cachier, H., Sciare, J. and Le Moullec, Y.: Characterization and contribution to PM<sub>2.5</sub> of semi-volatile aerosols in Paris (France), *Atmos. Environ.*, 41(36), 7969–7976, doi:10.1016/j.atmosenv.2007.09.031, 2007.

Freutel, F., Schneider, J., Drewnick, F., von der Weiden-Reinmüller, S.-L., Crippa, M., Prévôt, A. S. H., Baltensperger, U., Poulain, L., Wiedensohler, A., Sciare, J., Sarda-Estève, R., Burkhardt, J. F., Eckhardt, S., Stohl, A., Gros, V., Colomb, A., Michoud, V., Doussin, J. F., Borbon, A., Haeffelin, M., Morille, Y., Beekmann, M. and Borrmann, S.: Aerosol particle measurements at three stationary sites in the megacity of Paris during summer 2009: meteorology and air mass origin dominate aerosol particle composition and size distribution, *Atmospheric Chem. Phys.*, 13(2), 933–959, doi:10.5194/acp-13-933-2013, 2013.

Fröhlich, R., Crenn, V., Setyan, A., Belis, C. A., Canonaco, F., Favez, O., Riffault, V., Slowik, J. G., Aas, W., Aijälä, M., Alastuey, A., Artinano, B., Bonnaire, N., Bozzetti, C., Bressi, M., Carbone, C., Coz, E., Croteau, P. L., Cubison, M. J., Esser-Gietl, J. K., Green, D. C., Gros, V., Heikkinen, L., Herrmann, H., Jayne, J. T., Lunder, C. R., Minguillón, M. C., Močnik, G., O'Dowd, C. D., Ovadnevaite, J., Petralia, E., Poulain, L., Priestman, M., Ripoll, A., Sarda-Estève, R., Wiedensohler, A., Baltensperger, U., Sciare, J. and Prévôt, A. S. H.: ACTRIS ACSM intercomparison – Part 2: Intercomparison of ME-2 organic source apportionment results from 15 individual, co-located aerosol mass spectrometers, *Atmospheric Meas. Tech. Discuss.*, 8(2), 1559–1613, doi:10.5194/amtd-8-1559-2015, 2015.

Henry, R., Norris, G. A., Vedantham, R. and Turner, J. R.: Source Region Identification Using Kernel Smoothing, *Environ. Sci. Technol.*, 43(11), 4090–4097, doi:10.1021/es8011723, 2009.

Middlebrook, A. M., Bahreini, R., Jimenez, J. L. and Canagaratna, M. R.: Evaluation of Composition-Dependent Collection Efficiencies for the Aerodyne Aerosol Mass Spectrometer using Field Data, *Aerosol Sci. Technol.*, 46(3), 258–271, doi:10.1080/02786826.2011.620041, 2012.

Von Schneidemesser, E., Monks, P. S., Gros, V., Gauduin, J. and Sanchez, O.: How important is biogenic isoprene in an urban environment? A study in London and Paris: ISOPRENE IN AN URBAN ENVIRONMENT, *Geophys. Res. Lett.*, 38(19), doi:10.1029/2011GL048647, 2011.

# Two years of near real-time chemical composition of submicron aerosols in the region of Paris using an Aerosol Chemical Speciation Monitor (ACSM) and a multi-wavelength Aethalometer.

J.-E. Petit<sup>1,2,\*</sup>, O. Favez<sup>1</sup>, J. Sciare<sup>2</sup>, V. Cretn<sup>2</sup>, R. Sarda-Estève<sup>2</sup>, N. Bonnaire<sup>2</sup>, G. Močnik<sup>3</sup>, J.-C. Dupont<sup>4</sup>, M. Haeffelin<sup>4</sup>, and E. Leoz-Garziandia<sup>1</sup>

[1] : Institut National de l'Environnement Industriel et des Risques, Verneuil-en-Halatte, France

[2] : Laboratoire des Sciences du Climat et de l'Environnement (CNRS-CEA-UVSQ), CEA Orme des Merisiers, Gif-sur-Yvette, France

[3] : Aerosol d.o.o., Ljubljana, Slovenia

[4] : Laboratoire de Météorologie Dynamique, Institut Pierre Simon Laplace, Ecole Polytechnique, Palaiseau, France

\* now at Air Lorraine, 20 rue Pierre Simon Laplace 57000 Metz, France

Correspondence to: J.-E. Petit ([je.petit@air-lorraine.org](mailto:je.petit@air-lorraine.org))

## Abstract

Aerosol Mass Spectrometer (AMS) measurements have been successfully used towards a better understanding of non-refractory submicron (PM<sub>1</sub>) aerosol chemical properties based on short-term campaign. The recently developed Aerosol Chemical Speciation Monitor (ACSM) has been designed to deliver quite similar artefact-free chemical information but for low-cost, and to perform robust monitoring over long-term period. When deployed in parallel with real-time Black Carbon (BC) measurements, the combined dataset allows for a quasi-comprehensive description of the whole PM<sub>1</sub> fraction in near real-time. Here we present a 2-year long ACSM & BC datasets, between mid-2011 and mid-2013, obtained at the French atmospheric SIRTAs supersite being representative of background PM levels of the region of Paris. This large dataset shows intense and time limited (few hours) pollution events observed during wintertime in the region of Paris pointing to local carbonaceous emissions (mainly combustion sources). A non-parametric wind regression analysis was performed on this 2-year dataset for the major PM<sub>1</sub> constituents (organic matter, nitrate, sulphate and source apportioned BC) and ammonia in order to better refine their geographical origins and assess local/regional/advection contributions which information are mandatory for efficient mitigation strategies. While ammonium sulphate typically shows a clear advected pattern, ammonium nitrate partially displays a similar feature, but less expected, it also exhibits a significant contribution of regional and local emissions. Contribution of regional background OA is significant in spring and summer while a more pronounced local origin is evidenced



1 during wintertime which pattern is also observed for BC originating from domestic wood  
2 burning. Using time-resolved ACSM and BC information, seasonally differentiated weekly  
3 diurnal profiles of these constituents were investigated and helped to identify the main  
4 parameters controlling their temporal variations (sources, meteorological parameters). Finally,  
5 a careful investigation of all the major pollution episodes observed over the region of Paris  
6 between 2011 and 2013 was performed and classified in terms of chemical composition and  
7 BC-to-sulphate ratio used here as a proxy of the local / regional / advected contribution of  
8 PM. In conclusion, these first 2-year quality-controlled measurements of ACSM clearly  
9 demonstrate their great potential to monitor on a long term basis aerosol sources and their  
10 geographical origin and provide strategic information in near real-time during pollution  
11 episodes. They also support the capacity of the ACSM to be proposed as a robust and credible  
12 alternative to filter-based sampling techniques for long term monitoring strategies.

## 13 1. Introduction

14 The understanding of the formation and fate of atmospheric particulate pollution in urban  
15 areas represents sanitary, scientific, economic, societal and political challenges, greatly  
16 amplified by increasing media coverage of pollution episodes all around the world. Growing  
17 evidences of adverse health effects of atmospheric pollutants (Chow et al., 2006; Pope and  
18 Dockery, 2006; Ramgolam et al., 2009; WHO, 2012) are illustrated by the fact that ambient  
19 air pollution has been characterized as carcinogenic since December 2013 by the International  
20 Agency for Research on Cancer (IARC, 2013). However, the “aerosol cocktail effect”,  
21 directly linked to the complexity of the chemical composition and sources of the particulate  
22 phase, remains poorly understood.

23 In an effort to fill these lacks of knowledge, worldwide coordinated networking activities  
24 (such as Global Atmosphere Watch, European Monitoring and Evaluation Programme,  
25 AErosol RObotic NETwork) have been documenting, since decades, the chemical, physical  
26 and optical properties of aerosol pollution in various environments. At a European level, this  
27 effort is also supported by the Aerosols, Clouds and Traces gases Research InfraStructure  
28 network (ACTRIS) program which aims at pooling high quality data from state-of-the-art  
29 instrumentation such as the Aerosol Chemical Speciation Monitor (ACSM, Aerodyne  
30 Research Inc., Billerica, MA, USA).

31 The ACSM has been recently developed with the aim of robust and easy-to-use near real-time  
32 and artifact-free measurements of the major chemical composition of non-refractory  
33 submicron aerosol (Organic Matter,  $\text{NO}_3^-$ ,  $\text{SO}_4^{2-}$ ,  $\text{NH}_4^+$  and  $\text{Cl}^-$ ) on long-term basis (Ng et al.,  
34 2011). In parallel, a growing interest is also dedicated worldwide for the monitoring of Black  
35 Carbon (BC), considered as an adequate indicator of potential anthropogenic emission having  
36 sanitary impacts (Janssen et al., 2011). In particular, the use of 7-wavelength Aethalometer  
37 (Magee Scientific, USA) allows furthermore for BC source apportionment (Sandradewi et al.,  
38 2008), proven as robust over long term period (Herich et al., 2011). The combination of  
39 measurements from both instruments may thus constitute an efficient and relatively low-cost  
40 tool for the monitoring of submicron aerosol chemistry and a better knowledge of their  
41 phenomenology. Such strategy may be particularly useful to document aerosol sources and

Jean-Eudes Petit 15/1/15 23:43

Supprimé: versus

1 their geographical origin in large urban environments such as large urban areas which are  
2 characterized by a complex mixture of gaseous and particulate pollutions. Paris (France) is  
3 one of the largest European megacities and is rather isolated from other major urban  
4 environments. With ~11 million inhabitants, the Paris region accounts for 20% of total French  
5 population distributed over only 2% of its territory, leading to enhanced exposure to various  
6 types of pollution. Moreover, the flat orography of the Paris region favors pollution transport,  
7 making it representative of North-Western Europe aerosol pollution. AIRPARIF, the regional  
8 air quality monitoring network, recently estimated that, since 2007, about 2 million people per  
9 year have been exposed to poor air quality (referring to daily PM<sub>10</sub> concentrations European  
10 limit values; AIRPARIF, 2014) in this region. Over the past 7 years, annual PM<sub>2.5</sub>  
11 concentrations in Paris have remained quite stable although no continuous monitoring of the  
12 chemical composition of the particulate phase is available to investigate any trends in the  
13 major sources of fine aerosols.

14 A recent research program, based on a 1-year (2009-2010) daily filter sampling carried out at  
15 5 various sites (traffic, urban, suburban and regional background; Ghersi et al., 2010), was a  
16 unique opportunity to give insight into the seasonal variations, sources and geographical  
17 origins of aerosol pollution in the region of Paris (Bressi et al., 2013a,b; Petetin et al., 2013).  
18 However, long-term monitoring strategies based on the chemical analysis of aerosols sampled  
19 on filters are subject to various sampling and analytical artifacts (Appel et al., 1984; Turpin et  
20 al., 1994; Pathak et al., 2004; Cheng et al., 2009) and assumptions (OC-to-OM ratio for  
21 instance); they involve laborious laboratory analyses; they cannot capture processes  
22 governing diurnal variations of atmospheric pollutants and fail to provide rapid diagnostics  
23 during pollution events.

24 In this context, Aerosol Mass Spectrometer (AMS) techniques have provided extremely  
25 valuable information of artifact-free real-time chemical composition of submicron aerosols in  
26 urban areas over the past 10 years (Zhang et al., 2004, 2007; Jimenez et al., 2009). In Europe,  
27 OM and ammonium nitrate are generally the two main constituents of PM<sub>1</sub> (Zhang et al.,  
28 2007), showing, however, significant discrepancies during pollution episodes in terms of  
29 chemical composition. Real-time AMS data have improved the understanding of the physical  
30 and chemical (trans)formation pathways of both fractions, through the characterization of  
31 pollution dynamics and source apportionment analyses. Intensive field campaigns involving  
32 AMS measurements were performed during the 2009 summer and 2010 winter seasons in the  
33 frame of the European MEGAPOLI (Megacities: Emissions, urban, regional and Global  
34 Atmospheric POLLution and climate effects, and Integrated tools for assessment and  
35 mitigation) research program. They greatly improved the understanding of the sources and  
36 transformation processes of Paris aerosols, and especially its submicron organic fraction  
37 (Crippa et al., 2013a,b&c; Freutel et al., 2013; Healy et al., 2012; Laborde et al., 2013, Healy  
38 et al., 2013, Zhang et al., 2014). However, AMS techniques cost, size and intensive control  
39 requirements make them impractical for unattended monitoring. Nevertheless, they may still  
40 represent the best strategy to investigate specific trends in aerosol sources, especially in the  
41 context of elevated and stable PM concentrations as observed over the region of Paris during  
42 the past few years. In that perspective, the recently commercialized ACSM may represent an

interesting alternative and may ultimately represent the best strategy to deploy for long term monitoring of submicron aerosol sources and geographical origins.

As part of the ACTRIS project, a new in-situ atmospheric station has been implemented in 2011 at a background site of the region of Paris allowing the chemical, physical and optical characterization of submicron aerosol pollution at a regional scale. The key aim of the present paper is to describe and discuss one of the first long-term dataset obtained with the ACSM, offering opportunities for the evaluation of the scientific relevance of a new experimental strategy for long term monitoring of near real-time chemical composition of  $PM_{10}$ . Seasonal trends, wind sector analysis, diurnal variations and pollution episodes retrieved from a 2-year real-time measurement ACSM and BC datasets are presented and interpreted in order to refine the origins and parameters controlling the (trans)formation of particulate pollution over the region of Paris.

## 2. Material and methods

### 2.1 Sampling site and instrumentation

Long-term in-situ observations of the chemical, optical and physical properties of atmospheric aerosols have been initiated at SIRTa (Site Instrumental de Recherche par Télédétection Atmosphérique, <http://sirta.ipsl.fr>) since June 2011 within the EU-FP7 ACTRIS program (Aerosols, Clouds, and Traces gases Research InfraStructure Network, <http://www.actris.net>). Located 20 km Southwest of Paris (2.15° E, 48.71° N, 150 m above sea level) in a semi-rural area, this atmospheric supersite is representative of the regional background pollution over the region of Paris (Haeffelin et al., 2005; Crippa et al., 2013a).

The chemical composition of non-refractory submicron aerosol has been continuously monitored using a Quadrupole Aerosol Chemical Speciation Monitor (Aerodyne Research Inc.) which has been described in details by Ng et al., (2011). Briefly,  $PM_{2.5}$  aerosols are sampled at 3 L/min (from a  $PM_{2.5}$  cyclone inlet) and then sub-sampled at 85 mL/min (volumetric flow) through an aerodynamic lens, focusing submicron particles (40 nm - 1000 nm aerodynamic diameter, A.D.) onto a 600°C-heated conical tungsten vaporizer where non-refractory material are flash-vaporized and quasi-instantaneously ionized by electron impact at 70 eV. Fragments are detected following their mass-to-charge ratio by a quadrupole mass spectrometer. The procedure followed for the retrieval of chemical species concentrations from ACSM measurements is fully described in the Supporting Material. Briefly, the instrument calibration has been performed following the recommendation of Jayne et al. (2000) and Ng et al. (2011), where generated mono-disperse 300 nm A.D. ammonium nitrate particles are injected into both ACSM and Condensation Particle Counter (CPC) at different concentrations. Throughout the measuring period, three Response Factor (RF) calibrations and one  $(NH_4)_2SO_4$  calibrations were performed, summarized in Table 1. The low drift of the obtained slopes allowed the use of an average response factor of  $2.72 \cdot 10^{-11}$  (with an standard deviation of  $\pm 13\%$ ), as well as relative ion efficiencies (RIE) of 5.9, 1.2 and 1.4 for ammonium, sulphate and organic matter respectively, were used for the whole dataset.

Jean-Eudes Petit 5/11/14 15:58

Supprimé:  $NO_3^-$  ionization efficiency

1 Collection efficiencies were corrected using algorithms proposed by Middlebrook et al.  
2 (2012), and data were finally cross-validated using collocated PM<sub>1</sub> as well as PM<sub>2.5</sub> urban  
3 background measurements, retrieved from the regional association of air quality monitoring  
4 (AIRPARIF, <http://airparif.asso.fr>). The PM<sub>1</sub> and PM<sub>2.5</sub> datasets were obtained using Tapered  
5 Element Oscillating Microbalances (TEOM) equipped Filter Dynamic Measurements Systems  
6 (FDMS) as described by Grover (2005). A comprehensive determination of the overall  
7 uncertainty (as well as PM<sub>1</sub> components) associated to ACSM-derived measurements has  
8 been carried out in November 2013 through an inter-comparison exercise (Crenn et al., in  
9 preparation; Fröhlich et al., 2015). Here, the consistency of ACSM measurements has been  
10 assessed from the comparison with co-located measurements, as described in Section 3.

11 A total number of ~26,000 ACSM data points (with a temporal resolution of 30 min) were  
12 collected from June 2011 to June 2013 covering on average  $92 \pm 9\%$  of each month over this  
13 2-year period (it is to note that Sept-Oct 2012 and Feb-March 2013 were not taken into  
14 account within the latter calculation because the instrument was used for short-term intensive  
15 campaigns at other locations).

16 Aerosol light absorption coefficients  $b_{\text{abs}}$  were retrieved every 5 minutes from a 7-wavelength  
17 (370, 470, 520, 590, 660, 880 and 950 nm) AE31 Aethalometer from June 2011 to February  
18 2013, and from a 7-wavelength (370, 470, 520, 590, 660, 880 and 950 nm) AE33  
19 Aethalometer from February 2013 to May 2013. In both cases, instruments sampled aerosols  
20 with a PM<sub>2.5</sub> cut-off inlet, operating at 5 L/min. Filter-based absorption measurements need to  
21 be compensated for multiple scattering in the filter matrix and for loading effects, using  
22 mathematical algorithms (Collaud Coen et al., 2010). While AE31 data were compensated  
23 using the corrections of Weingartner et al. (2003) as described in Sciare et al. (2011), the use  
24 of the Dual-Spot Technology® in the AE33 avoids the need of manual post-processing to  
25 compensate the data (Drinovec et al., 2014). Both instruments performed absorption  
26 measurements simultaneously during 7 days in February 2013 (Fig. S1a). Absorption  
27 coefficients at 880 nm showed a slope of 0.93 and a very satisfactorily  $r^2$  (0.96,  $n=3,023$  of 5-  
28 min data points). Black Carbon concentrations for the whole (2-year) dataset were then  
29 calculated from the absorption coefficient at 880 nm, with a mass absorption cross-section  
30 (MAC) of  $8.8 \text{ m}^2/\text{g}$  (Fig. S1b), determined from the comparison with collocated filter  
31 measurements of elemental carbon (EUSAAR2 thermo-optical protocol, Cavalli et al., 2010).  
32 This value is close to the default input value implemented in the AE33 at 880 nm ( $7.77 \text{ m}^2/\text{g}$ ).  
33 Although still under discussion (Bond and Bergstrom, 2006; Cappa et al., 2012), such  
34 relatively high MAC values might be related to a possible encapsulation of soot particle by  
35 organic/inorganic compounds at our regional background site and to the presence of BC from  
36 wood burning emissions during wintertime, both leading to an increase of BC mass  
37 absorption efficiency (Liousse et al., 1993; Bond and Bergstrom, 2006; Lack et al., 2008). A  
38 total number of ~280,000 BC data points (~133,000 5-min points from AE31 and ~147,000 1-  
39 min points from AE33) were collected from June 2011 to June 2013.

40 Ammonia measurements during selected periods (mainly during the spring, winter and  
41 summer seasons) were carried out using an AiRRmonia (Mechatronics Instruments BV, The  
42 Netherlands). Based on the conductimetric detection of ammonium, gaseous ammonia is

Jean-Eudes Petit 19/1/15 11:52  
Supprimé: (30-min)

Jean-Eudes Petit 6/11/14 11:53  
Supprimé: in prep

sampled at 1 L/min through a sampling block equipped with an ammonia-permeable membrane; a water counter-flow allows ammonia to solubilize in ammonium. A second purification step is applied by adding 0.5 mM sodium hydroxide, leading to the detection of ammonium in the detector block. The instrument has been calibrated regularly using solutions of 0 ppb and 500 ppb of ammonium. Two sets of sampling syringes ensure a constant flow throughout the instrument, but also create a temporal shift, estimated at 20 to 40 min by different studies (Cowen et al., 2004; Zechmeister-Boltenstern, 2010). In our case, this shift was set at 30 min.

Pre-fired 47-mm diameter quartz filters were sampled in PM<sub>2.5</sub> at the same location using a low-volume (1m<sup>3</sup>/h) sampler (Partisol Plus, Thermo Environment) equipped with a volatile organic compounds active charcoal denuder. Four-hour filters and 24-h filters were discontinuously sampled respectively from 10 Feb. 2012 to 02 Mar. 2012 and during the period from August 2012 to April 2013. These filters were analyzed for their water-soluble inorganic (anions and cations) and elemental/organic carbon contents using respectively Ion Chromatography and Sunset OC/EC analyzer (EUSAAR2 thermal protocol), accordingly to Sciare et al. (2008) and Cavalli et al. (2010).

Finally, standard meteorological parameters (Temperature, Relative Humidity, Wind Speed and Direction) were obtained from continuous measurements at Ecole Polytechnique, located 4 km East of our station with an A100R Campbell Scientific cup anemometer for wind speed and a W200P weathervane for wind direction, at 10 m above ground level. Additionally, the Boundary Layer Height (BLH) was derived from Pal et al. (2013) methodology. The attribution of the BLH was processed in combining diagnostic of the surface stability from high frequency sonic anemometer measurements and LIght Detection and Ranging (LIDAR) attenuated backscatter gradients from aerosols and clouds.

All measurements presented here are expressed in Coordinated Universal Time (UTC).  
Seasons are differentiated upon seasonal equinoxes.

## 2.2 Urban background PM<sub>2.5</sub> measurements

Within the framework of mandatory air quality monitoring, urban background measurements are continuously being carried out in the region of Paris. Hourly PM<sub>2.5</sub> data from TEOM-FDMS measurements were retrieved from the three stations representative of the Paris urban background (namely Bobigny, Gennevilliers and Vitry-sur-Seine). Datasets are available online upon request on <http://airparif.asso.fr>.

## 2.3 Backtrajectories and Non-parametric Wind Regression

To illustrate air mass origin during specific pollution episodes, 72-h backtrajectories were calculated every 3 hours from the PC based version of Hysplit (Draxler, 1999) with GDAS

1 meteorological field data. Backtrajectories were set to end at SIRTa coordinates (48.71°N,  
2 2.21°E) at 100 m above ground level.

3 Non-parametric Wind Regression (NWR) is a smoothing algorithm (Henry et al., 2009) to  
4 alternatively display pollution roses, and has been already successfully applied to various  
5 atmospheric pollutants and pollution sources (Yu et al., 2004; Pancras et al., 2011; Olson et  
6 al., 2012). The objective is to estimate the concentration of a pollutant given any ( $\theta$ ,  $v$ ) couple  
7 (wind direction and speed, respectively), from measured wind speed and direction, and  
8 concentration.

$$E(\theta|\vartheta) = \frac{\sum_{i=1}^N K_1\left(\frac{\theta - W_i}{\sigma}\right) \cdot K_2\left(\frac{\vartheta - Y_i}{h}\right) \cdot C_i}{\sum_{i=1}^N K_1\left(\frac{\theta - W_i}{\sigma}\right) \cdot K_2\left(\frac{\vartheta - Y_i}{h}\right)}$$

9 Where  $E$  is the concentration estimate at a wind direction  $\theta$  and speed  $v$ ;  $W_i$ ,  $Y_i$  and  $C_i$  the  
10 wind direction, speed and atmospheric concentrations, respectively, measured at  $t_i$ ;  $\sigma$  and  $h$   
11 the smoothing factors; and  $K_1$  and  $K_2$  two kernel smoothing functions defined as:

$$K_1(x) = \frac{1}{\sqrt{2\pi}} \cdot e^{-0.5 \cdot x^2}, -\infty < x < \infty$$

$$K_2(x) = 0.75 \cdot (1 - x^2), -1 < x < 1 = 0$$

12 The choice of the two smoothing factors  $\sigma$  and  $h$  can be carried out using statistical  
13 calculations, although its empirical determination stays feasible, as final interpretation should  
14 not be changed. Here,  $\sigma$  and  $h$  were set to 7 and 1.5, similarly to Petit et al. (2014). Finally,  
15 the equivalent of the wind rose is calculated from the probability density:

$$f(\theta, \vartheta) = \frac{1}{N\sigma h} \cdot \sum_{i=1}^N K_1\left(\frac{\theta - W_i}{\sigma}\right) K_2\left(\frac{\vartheta - Y_i}{h}\right)$$

16 where  $N$  is the total number of points.

17 Due to higher measurement uncertainties in wind direction at low speeds, data associated with  
18 wind speeds lower than 1 m/s were discarded, potentially inducing an underestimation of very  
19 local pollution events.

20

## 21 **2.4 Source apportionment of carbonaceous aerosols**

22 The measurement of aerosol absorption at multiple wavelengths is allowing for BC source  
23 apportionment. Organic molecules, especially Polycyclic Aromatic Hydrocarbons and Humic-  
24 Like Substances, strongly absorb in the UV and blue part of the light spectrum. Based on the  
25 fact that these compounds are primarily related to biomass combustion, the deconvolution of  
26 BC into two contributions: fuel fossil and wood burning ( $BC_{ff}$  and  $BC_{wb}$ , respectively) can be  
27 carried out (Sandradewi et al., 2008). Such source apportionment has already been

successfully performed during intensive field campaigns as well as for long-term monitoring periods, frequently enlightening the significant contribution of wood burning to ambient BC concentrations during wintertime (Favez et al., 2009, 2010; Sciare et al., 2011, Herich et al., 2011; Crippa et al. 2013a). Here, the 470 nm and 880 nm channels were used, with an absorption Ångström exponent of 2.1 and 1.0 for pure wood burning and traffic, respectively, similarly to previous work focusing on the February-March 2012 period of the same dataset (Petit et al., 2014).

The source apportionment of our organic aerosol data is not presented here although Positive Matrix Factorization applied to AMS or ACSM database is an efficient tool for the identification of organic aerosol primary sources and secondary formation processes (see for instance Lanz et al., 2007; Jimenez et al. 2009; El Haddad et al., 2013; Carbone et al., 2013; Bougiatioti et al., 2014; Petit et al. 2014). Such a work will be reported elsewhere (Crenn et al., in prep.) as important issues related to the seasonal variation of specific organic aerosol factor profiles have to be addressed in many details with a lot of sensitivity tests which are beyond the objectives of the present study.

### 3. Cross-validation of particulate chemical species concentrations

Fig. 1 illustrates the temporal variations of chemical species concentrations used for the present study from June 2011 to May 2013. This extended duration highlights the robustness of used instruments, and in particular the ACSM which did not undergo any major failures over this 2-year period. The consistency of the concentrations of each chemical constituent retrieved from the ACSM has been checked via comparisons with filter measurements (Fig. 2) as well as a chemical mass closure of  $PM_{10}$  (Fig. 3).

ACSM nitrate is very consistent with filter measurements, the slope of the linear regression being close to 1 ( $r^2=0.85$ ,  $N=147$ ). No overestimation of ACSM nitrate is observed at high concentrations, which suggests the ability of the Middlebrook algorithm to properly correct our ACSM collection efficiencies. Higher discrepancies are observed for sulphate. This feature has already been mentioned in previous studies for ACSM (Ng et al., 2011; Budisulistiorini et al., 2014), and AMS instruments (Takegawa et al., 2005). This could be partly related to the size distribution of sulphate, as fine ( $PM_{2.5}$ ) sulphate can partially be associated with submicron sea salt and/or dust particles. Fine ammonium sulphate aerosols originating from secondary processes and long-range transport (Sciare et al., 2010; Freutel et al., 2013) may also present a larger size mode extending above  $1\text{ }\mu\text{m}$  and partially not sampled by the ACSM. A sulphate ion efficiency calibration was also performed in May 2013 to investigate possible change in RIE, but no significant discrepancy from the default value of 1.2 was found.

The OM-to-OC ratio obtained from the comparison between ACSM and filter-based measurements exhibits a mean value of approximately 1.5, which is lower than the value recommended for urban areas ( $1.6 \pm 0.2$ , Turpin and Lim, 2001) and 33% lower than and/or equal to values used in Paris metropolitan area in previous studies ( $\sim 2$  in Bressi et al., 2013;

Jean-Eudes Petit 6/11/14 17:16

Supprimé: firstly

1.6 in Sciare et al., 2010). Although this ratio is subject to caution, by virtue of potential geographical and temporal discrepancies, the relatively low value observed here might be explained by the presence of organic material between 1 and 2.5  $\mu\text{m}$  as well as filter sampling artifacts.

A chemical mass closure exercise, where the combination of validated ACSM and Aethalometer data is compared to co-located  $\text{PM}_{10}$  TEOM-FDMS measurements, was used to assess the capacity of the two former instruments to correctly describe the  $\text{PM}_{10}$  fraction over long-term periods. For this purpose, the reconstructed  $\text{PM}_{10}$  ( $\text{PM}_{\text{chem}}$ ) introduced here corresponds to the sum of all non-refractory species measured by the ACSM ( $\text{OM}$ ,  $\text{NO}_3^-$ ,  $\text{SO}_4^{2-}$ ,  $\text{NH}_4^+$  and  $\text{Cl}^-$ ) and Black Carbon measured by Aethalometer, and is assumed to quasi-exhaustively account for submicron aerosols (Putaud et al., 2004).  $\text{PM}_{\text{chem}}$  daily averages were compared to the TEOM-FDMS dataset, since the latter instrument is considered as equivalent to the gravimetric reference method on this temporal scale. From June 2011 to May 2013, the 341-point (this number being due to the combined availability of ACSM, BC and PM data) scatter plot shows a very satisfactory correlation coefficient ( $r^2=0.85$ ) with a slope of 1.06.

#### 4. Representativeness of our 2-year observation period

Monthly mean atmospheric conditions were compared to standard meteorological parameters in order to investigate any anomalies over the 2011-2013 period (Fig. 4). Temperature, rainfall and sun exposure representative for the region of Paris were retrieved from monthly weather reports available at <https://donneespubliques.meteofrance.fr>, and are calculated from a 30-year period (1981-2010) (Arguez and Vose, 2011). A similar study was also performed for particulate matter concentrations, with representative  $\text{PM}_{2.5}$  defined as the average  $\text{PM}_{2.5}$  concentrations calculated from 2007 to 2014 at the three historical Airparif urban background stations.

Briefly, autumn 2011 was relatively mild,  $\text{PM}_{2.5}$  levels being close to representative concentrations for the period. The end of winter 2011-2012 and early spring 2012 were particularly dry and sunny, enabling enhanced photochemical transformation and exhibited unusually high  $\text{PM}_{2.5}$  concentrations in February and March 2012. The summer 2012 was chilly and rainy, especially in June 2012, leading to lower  $\text{PM}_{2.5}$  levels (Yiou and Cattiaux, 2013). Finally, the first two months of 2013 were unusually cold, whereas March 2013 was remarkably representative of wintertime conditions. The highest observed discrepancies occur with highest measured mass, which may highlight an intensification of pollution episodes. On a broader perspective, this feature is also observed through inter-annual variability of urban background  $\text{PM}_{2.5}$  concentrations (Fig. S2). This underlines the need of continuous monitoring over several year periods. Interestingly, no direct link can be drawn between meteorological anomalies and unusual high  $\text{PM}_{2.5}$  concentrations. Indeed, while the high  $\text{PM}_{2.5}$  levels observed in Feb. 2012 and March 2012 may be linked to unusual low temperatures, exceptionally high temperatures can also be associated with high  $\text{PM}_{2.5}$  concentrations. This has to be related to the seasonal variability of sources, origins and

Jean-Eudes Petit 5/11/14 15:36

**Supprimé:** Moreover, significant discrepancies occur from one year to another, where highest averages show highest standard deviations (Fig. S2).



(trans)formation pathways; and is being investigated within the following sections, taking advantage of long-term trend analysis, wind regression, diurnal variations, and the analysis of pollution episodes.

Finally, it should be underlined that the Paris region is mostly influenced by winds coming from the Southwest (Fig. 5) sector. This sector is characterized by clean air masses from the Atlantic Ocean with high wind speeds, and is usually associated with low PM concentrations. The Northeast wind sector exhibits a smaller occurrence than previously observed between Sept. 2009 and Sept. 2010 (Supplementary information of Bressi et al., 2013).

## 5. Long-term trend and general features

2-year temporal variations of the chemical composition of submicron aerosols (OM,  $\text{NO}_3^-$ ,  $\text{SO}_4^{2-}$ ,  $\text{NH}_4^+$ ,  $\text{Cl}^-$ ,  $\text{BC}_{\text{fr}}$  and  $\text{BC}_{\text{wb}}$ ) and ammonia ( $\text{NH}_3$ ) are presented in Fig. 1. Similarly to Bressi et al. (2013), a clear seasonal pattern is observed here, with highest concentrations observed during winter and early spring while summer periods exhibit the lowest pollution levels (Fig. 6a), which is also consistent with general patterns observed in Northern Europe (Barmpadimos et al., 2012; Waked et al., 2014). Regardless of the season, OM dominates the  $\text{PM}_{10}$  chemical composition, followed by ammonium nitrate whose contribution is highest during spring, a feature that is generally observed for European urban areas (Zhang et al., 2007; Putaud et al., 2010). Fig. 6b presents the binned major chemical composition and the frequency per season of data points as a function of  $\text{PM}_{10}$  concentration levels. The contribution of Secondary Inorganic Aerosols (SIA, mostly  $\text{NO}_3^-$ ,  $\text{SO}_4^{2-}$  and  $\text{NH}_4^+$ ) increases with the increases of  $\text{PM}_{10}$  mass until  $50 \mu\text{g}/\text{m}^3$ , highlighting the role of inorganic secondary pollution during spring months (Fig. 6b). This well-documented pattern that has already been reported for the region of Paris in several studies (see for instance Sciare et al., 2010 and Bressi et al., 2013a). Very interestingly, above  $50 \mu\text{g}/\text{m}^3$ , organic contribution, as well as wintertime frequency, increases to dominate the chemical composition of the highest measured  $\text{PM}_{10}$  concentrations with an associated increase in BC, a feature which has not been seen during the AIRPARIF-Particules projects, essentially due to highly time resolved measurements, nor investigated during the MEGAPOLI project. There are well defined occurrences of high concentrations (~150 data points of 30 min) suggesting sharp pollution events with a limited temporal duration; contradictorily to the 20-50  $\mu\text{g}/\text{m}^3$  mass class presenting much more data points that highlight either a higher frequency of sharp events and/or pollution episodes with a longer temporal duration.

We have used here the  $\text{BC}/\text{SO}_4$  ratio to assess potential transport of pollution. Sulphate mainly forms through heterogeneous processes with a slow kinetic rate and spreads over large scales (Putaud et al., 2004). For that reason, it can be considered as a good indicator of long-range transport assuming minor local  $\text{SO}_2$  sources (background annual  $\text{SO}_2$  concentrations of about  $2 \mu\text{g}/\text{m}^3$  in the region of Paris; AIRPARIF, 2014). On the contrary, Black carbon in the region of Paris shows an important gradient from the city center to regional background (Bressi et al., 2013a) and can be used to better infer local (Paris city) influence at our background station. Although in-situ sulphate formation may occur (for instance during fog

Jean-Eudes Petit 5/11/14 15:38

Supprimé: the Megapoli nor

1 episodes; Healy et al., 2012) and long range transport of BC may be observed over the region  
 2 of Paris (Healy et al., 2012 and 2013), as a whole, the use of the BC/SO<sub>4</sub> ratio may support  
 3 | our study on local / regional / advected pollution. As shown in Fig. 7, the BC/SO<sub>4</sub> ratio  
 4 decreases along with the increase of PM<sub>1</sub> (and thus secondary ions mass fraction), suggesting  
 5 | potential regional and/or trans-boundary transport, and large-scale pollution episodes, as  
 6 previously reported by several studies in Northern France (Bessagnet et al., 2005; Sciare et  
 7 al., 2010; Bressi et al., 2013; Waked et al., 2014; Freutel et al., 2013). Very interestingly, this  
 8 BC/SO<sub>4</sub> ratio dramatically increases for the highest concentrations, where the concomitant  
 9 increases of the Ångström exponent, of the contribution of BC<sub>wb</sub> relatively to BC, along with  
 10 | the increase of OM and wintertime frequency (Fig. 7), suggest intense local and/or regional  
 11 wood burning pollution episodes during winter. Moreover, except the single wood-burning  
 12 episode observed on 5 Feb. 2012 (described in Petit et al., 2014) all these intense PM  
 13 pollution peaks (PM<sub>1</sub> > 60 µg/m<sup>3</sup>) also occurred in most of the rural/suburban/urban  
 14 AIRPARIF monitoring stations. This pattern underlines homogeneous meteorological  
 15 conditions over the region of Paris with “local” emissions being measured at a regional scale  
 16 | (within a distance of at least 50 km from the city center).

17

## 18 6. Seasonality and insights on geographical origins

19 Fig. 8 displays the Wind Regression analysis plots for species of interest, naming OM, NO<sub>3</sub><sup>-</sup>,  
 20 SO<sub>4</sub><sup>2-</sup>, NH<sub>3</sub>, BC<sub>ff</sub> and BC<sub>wb</sub>.

21 Overall, OM concentrations do not exhibit a particular dependence on wind direction, the  
 22 regional background always staying at a significant contribution throughout seasons (~ 3-6  
 23 µg/m<sup>3</sup>). However, higher OM concentrations occurred in autumn and winter and are  
 24 associated with very low wind speeds suggesting higher local influence together with higher  
 25 local wood burning emissions (as previously suggested from Fig. 6b and 7). During summer,  
 26 OM concentrations are lower (by a factor of ~2.2) and show a more homogeneous  
 27 distribution (e.g. with lower local influences).

28 As expected, semi-volatile nitrate concentrations are higher during the coldest months (in  
 29 spring and winter). They are associated with relatively high wind speeds (~20 km/h) coming  
 30 from the N and NE direction, suggesting significant medium-to-long-range transport of  
 31 ammonium nitrate during these seasons which is consistent with similar observations reported  
 32 for the region of Paris (Bressi et al., 2013a; Freutel et al., 2013; Petetin et al., 2013).  
 33 However, the significant nitrate concentrations observed for all the range of wind speed from  
 34 the N-NE direction suggest, at least for the lowest wind speed, a significant contribution of  
 35 the region of Paris. Possible impacts of industrial activities in the Seine estuary (i.e. Rouen,  
 36 Le Havre), especially during spring, may also be responsible for the noticeable nitrate hotspot  
 37 observed in the NW sector. In autumn, nitrate concentrations are higher at low wind speeds,  
 38 in agreement with the fact that traffic emissions are slightly higher in September and October  
 39 than the rest of the year in Paris (V-Trafic report, 2014), and that BC<sub>ff</sub> concentrations are also  
 40 the highest during these months. This is also consistent with a relatively fast nitrate formation  
 41 mechanism from local NO<sub>x</sub> emissions as reported by Petetin et al. (2013).

Jean-Eudes Petit 15/1/15 11:14

Supprimé: versus

Jean-Eudes Petit 15/1/15 11:14

Supprimé: transported

Jean-Eudes Petit 15/1/15 23:46

Supprimé: /

Jean-Eudes Petit 15/1/15 23:46

Supprimé: /

Sulphate features different behaviour than nitrate, where the non-local origin is much more pronounced. High concentrations are associated with high wind speeds originating from the NNE, leading to the same conclusions as those reported in the literature on the major role of long range transport of this compound (Pay et al., 2012; Bressi et al., 2013b; Petetin et al., 2013; Waked et al., 2014). Petrochemical and shipping activities may explain the observed hotspot in the marine NW sector, especially noticeable in spring, which may be linked with meteorological conditions enhancing ammonium sulphate formation and transport.

The region of Brittany, located less than 300 km West of the region of Paris, is the principal emitter of ammonia in France through intense agricultural activities (<http://prtr.ec.europa.eu/DiffuseSourcesAir.aspx>). However, no clear contribution from this region is observed from our wind regression analysis. This may be partly related to very few occurrences of air masses passing over Brittany and reaching the region of Paris. Despite hotspots from the NE/E in spring, or from the N/NE in winter, no clear wind sector is directly responsible for high  $\text{NH}_3$  concentrations at our station, suggesting a diffuse regional source for this compound.

In Europe,  $\text{BC}_{\text{ff}}$  is assumed to be an excellent tracer of traffic emissions in urban areas (Herich et al., 2011 for instance). Although long range transported  $\text{BC}_{\text{ff}}$  may not be excluded as shown by Healy et al. (2012, 2013), here, wind regression analyses show that high  $\text{BC}_{\text{ff}}$  concentrations occurred at low wind speeds, highlighting the importance of local/regional traffic emissions in the Paris region, especially during the autumn and winter seasons. In spring, a clear distribution over a large range of wind speeds is noticeable in the NNE wind sector. This is consistent with the fact that Paris city is located NNE from our station (e.g. higher contribution of the Paris city plume to measured  $\text{BC}_{\text{ff}}$  concentrations at SIRTa). This is also related to a higher occurrence of this wind sector during spring.

Black Carbon from biomass burning combustion ( $\text{BC}_{\text{wb}}$ ) presents a clear seasonal trend similar to OM, with the highest concentrations during cold seasons at low wind speeds, suggesting increasing local influence in wood burning emissions. The lowest boundary layer heights (BLH) observed during wintertime favouring the accumulation of pollutants at ground level together with the large contribution of individual (domestic) wood burning sources homogeneously spread over the region of Paris may explain the significant contribution of regional emissions observed during winter.

Finally, it should be noted that the geographical origin of each investigated chemical constituent remains globally unchanged throughout the year with a well-defined sectorized location. While SIA and  $\text{BC}_{\text{ff}}$  fractions are mainly associated with the NNE sector (coming from Paris City and/or further away), highest OM and  $\text{BC}_{\text{wb}}$  concentrations exhibit strong local NW and SE sectors origins. Various sources of organic matter also contribute to a significant contribution of the (unsectorized) regional background.

## 7. Weekly diurnal profiles and insight on sources and processes

1 Near real-time observations over long-term periods offer a unique opportunity to provide  
2 robust diurnal profiles for each season. First, Fig. 9 shows the average diurnal profiles of  
3 ambient temperatures (Fig. 9a) and BLH (Fig. 9b) across seasons. Weekly diurnal profiles for  
4 OM,  $\text{NO}_3^-$ ,  $\text{NH}_4^+$ ,  $\text{NH}_3$ ,  $\text{BC}_{\text{ff}}$  and  $\text{BC}_{\text{wb}}$  are presented for different seasons from hourly  
5 averages (Fig. 10). Sulphate variations are not presented and discussed here because they lead  
6 to poor daily variations (average of  $0.75 \mu\text{g}/\text{m}^3 \pm 2\%$ ), which are consistent with its mid-to-  
7 long range transport origin.

8 Clear weekly and diurnal patterns can be observed for carbonaceous aerosols. Independently  
9 to the investigated season,  $\text{BC}_{\text{ff}}$  presents a well-marked bimodal diurnal profile, with maxima  
10 in the morning (starting at 06:00 UTC) and the evening (starting at 17:00). This reflects the  
11 proximity of the traffic source (with daily commuting) and dilution in the boundary layer  
12 during daytime (Fig. 9b). With an average of  $0.61 \mu\text{g}/\text{m}^3$ , weekdays exhibit slightly higher  
13 concentrations than weekends ( $0.51 \mu\text{g}/\text{m}^3$  on average). By comparison, the diurnal variability  
14 of  $\text{BC}_{\text{wb}}$  is revealed only in autumn and winter, with the combination of enhanced wood  
15 burning emissions, low temperatures and BLH (Fig. 9), leading to a unimodal pattern with  
16 increasing concentrations after 18:00 UTC. Although individual wood-burning stoves only  
17 represent around 5% of the means of heating in the region of Paris, they contribute to almost  
18 90% of  $\text{PM}_{10}$  residential emissions in the region of Paris (Airparif emission inventory for the  
19 year 2010; Airparif, 2013) and are likely to represent the major contributor to  $\text{BC}_{\text{wb}}$ .

20 For OM, highest variations (in terms of concentration amplitude) are observed during autumn  
21 and winter, with a growing influence of wood-burning heating, as OM concentrations nicely  
22 follow  $\text{BC}_{\text{wb}}$  ones. Levels of both compounds during the evening are approximately 20%  
23 higher during weekends than during weekdays. More specifically, low BLH in winter  
24 (Fig. 9b) increase measured concentrations, leading, for example, to morning OM peaks that  
25 should be linked to traffic emissions. By contrast, the diurnal profile is rather flat with poor  
26 temporal variations in summer and is accordance with the homogeneous geographical  
27 distribution from NWR calculation for this season. The lack of decrease in the afternoon  
28 during weekdays suggests rapid formation of secondary organic aerosols (SOA) from diverse  
29 anthropogenic (traffic for instance, as underlined by Platt et al., 2013 and Nordin et al., 2013)  
30 and biogenic sources (Carlton et al., 2009). During spring, OM globally follows the variations  
31 of nitrate, highlighting fast displacements of gas-particle equilibriums of semi-volatile  
32 material due to meteorological conditions. Some peaks are observed some days during the  
33 night, which could underline the residual contribution of wood burning emissions in March  
34 and April.

35 For SIA, nitrate and ammonium display very similar diurnal and weekly profiles, illustrating  
36 the importance of ammonium nitrate by comparison with ammonium sulphate. Both  
37 compounds display well-marked diurnal profiles with maximum at night (especially in  
38 autumn and winter) and/or early morning (especially in spring and summer), which has to be  
39 related to the enhancement of ammonium nitrate formation under low temperature and/or high  
40 relative humidity. The temporal variations of the two compounds can also be linked to the one  
41 of ammonia. For instance, during summertime, ammonia presents unimodal diurnal profiles,  
42 with highest values around noon, and nicely follows temperature (Fig. 9a), in good agreement

with previous studies (Bari et al., 2003; Lin et al., 2006). This phenomenon is exactly opposite to the variations of ammonium and nitrate exhibiting unimodal pattern with highest concentrations during the night. Meteorological conditions can then fully explain the formation/partitioning of SIA as well as ammonia concentration during summer.

Interestingly however, ammonia shows different profiles as a function of the season. In particular, during springtime, this compound displays a clear bimodal profile, with a morning and an evening peak, concomitant with traffic emissions and that come over elevated regional background levels due to the use of nitrogen-containing fertilizers in this period of the year. However, this bimodal pattern is not observed during the summer and winter seasons, where traffic also occurs. Although traffic-related ammonia has already been reported in urban environments (Edgerton et al., 2007; Pandolfi et al., 2012; Saylor et al., 2010) and several studies raising concerns about uncontrolled ammonia emissions from De-NO<sub>x</sub> systems (Baum et al., 2001; Heeb et al., 2006 and 2012 for instance), this spring bimodal profile may also be related to other parameters than traffic emissions. Indeed, as already described by Bussink et al. (1996), emission of ammonia can occur during the evaporation of the morning dew, especially when soils are loaded with fertilizers. The morning decrease observed for ammonia in spring can then be associated with the growing of the mixing depth layer (Fig. 9b) while, in the afternoon ammonia increases may be partly explained by temperature driven gas-phase partitioning changes of ammonium nitrate.

## 8. PM<sub>1</sub> pollution episodes over the region of Paris

An in-depth characterization of each pollution episodes over the region of Paris is particularly important in the context of mitigation policies which are usually taken at a local scale during these episodes. Such investigation should provide useful information regarding PM (trans)formation processes and help identifying parameters influencing the temporality of their chemical composition.

Statistical representativeness of pollution episodes (duration and intensity) may be addressed using our long-term datasets. Based on our 2-year dataset, the highest 1% of observed PM<sub>1</sub> concentrations ( $q_{99} \sim 49 \mu\text{g}/\text{m}^3$ , representing around 200 data points of 30min; i.e. approximately 100h) mostly occur during February, April and November, while persistent pollution episodes (PM<sub>1</sub> > 20  $\mu\text{g}/\text{m}^3$  during at least 3 consecutive days) mostly occur in early Spring. More interestingly, the majority of the highest PM<sub>1</sub> concentrations fall within these persistent pollution episodes. As previously suggested from higher BC/SO<sub>4</sub> ratios (Section 5 and Fig. 7), the highest PM<sub>1</sub> concentration peaks are associated with rather local emissions. This result clearly points to the contribution of local/regional emissions during persistent pollution episodes. A more detailed analysis (episode-by-episode) is performed in the following to better characterize the local/regional versus advected PM pollution during persistent pollution episodes.

Eight persistent pollution episodes (PM<sub>1</sub> > 20  $\mu\text{g}/\text{m}^3$  during at least 3 consecutive days) were detected between mid-2011 to mid-2013 and are displayed in Table 2 and Fig. 12&13. Fig. 12

Jean-Eudes Petit 6/11/14 11:52

Supprimé: 1

shows the averaged  $PM_1$  chemical composition (in  $\mu g/m^3$ ) for each episode, chronologically numbered, from 1 to 8. Table 2 summarizes key information for each episode. Fig. 13 shows air masses origins, wind rose and temporal variations of the chemical composition of each episode. As a general pattern for each episode, the chemical composition of  $PM_1$  is dominated by OM and/or ammonium nitrate. Sulphate presents the highest variability (concentration standard deviation of 53% over all episodes) compared to OM and nitrate (~30%), possibly suggesting various contributions of advected pollution.

The following provides a thorough description of each episode.

Episode 1 (19/11/2011 – 24/11/2011): While winds come from the NW and E sectors, 72h-backtrajectories originate from SSE and exhibit a recirculation over a part of the Northern France. Moreover, along with the  $BC/SO_4$  ratio (3.56; e.g. the highest of all episodes), and a low BLH with no significant variations, the chemical composition is largely dominated by OM (60.8% of  $PM_1$ ), suggesting significant local influence. The contribution of  $BC_{wb}$  remains insignificant compared to  $BC_{ff}$ , which could underline the accumulation in the atmosphere of fossil-fuelled combustion sources (notably illustrated by the very low altitude of the air masses ending on the 21 and 23 Nov).

Episode 2 (05/02/2012 – 13/02/2012): This episode presents two distinct phases. At the beginning, air masses come from the SE but originating from the E at low altitudes; along with very low temperatures (below  $0^\circ C$  all day), high OM and BC concentrations and  $BC/SO_4$  ratio (average of 22.6 and  $0.6 \mu g/m^3$ , and 2.7, respectively from 5 to 8 Feb.). This is related to an intense local wood-burning episode, already thoroughly described in Petit et al. (2014). Then, from the 8 Feb, winds and air masses originate from NNE and secondary inorganic ions, especially ammonium nitrate, dominate the chemical composition. The associated wind speed may underline mid- to long-range transport, although the impact of the Paris plume cannot be excluded here.

Episode 3 (29/02/2012 – 03/03/2012): Along with this pollution episode, trajectories have rapidly changed in origin but have remained low in altitude. The RH remained very high, reaching 100% most of the time. Very interestingly, concentrations dropped on 01/03 and 03/03 during the beginning of the day, coinciding with two stratus lowering fog events. These two fog events occurred during the second half of the night, and evaporated as the sun rose. The influence of fogs regarding the chemical transformation of  $PM_1$  is notably highlighted by higher sulphate concentrations just after the evaporation of the first fog (and also when trajectories flew over the English Channel and Belgium), which could suggest transported  $SO_2$  and oxidation over the region of Paris enhanced by fast fog processing (Kai et al., 2007; Rengarajan et al., 2011).

Episode 4 (12/03/2012 – 17/03/2012): Winds have originated from all directions (but mostly from NNE) suggesting anticyclonic conditions. The first half of the period exhibits rather stable chemical composition (dominated by ammonium nitrate) and clear diurnal variations of RH, T and BHL. Then, after 15/03, daily amplitudes of the following 3 meteorological parameters increased: T reached  $20^\circ C$ , RH 30% and BHL 1000 m, compared to the first half where they reached  $15^\circ C$ , 50% and 600m, respectively. This caused rapid decreases of

concentrations, due to higher temperature amplitudes enhancing the gas partitioning of semi-volatile material, and an increase of BLH allowing the dilution of atmospheric pollutants.

Episode 5 (23/03/2012 – 26/03/2013): Air masses originated from the NE to the E, and winds from the N to the NE. This episode is characterized by the strong diurnal variation of OM and ammonium nitrate, due the high amplitude of the BLH and temperatures going above 15°C, similarly to the previous episode. The high average BC/SO<sub>4</sub> ratio (2.37) is not representative of its temporality; the highest values are observed for lowest PM concentrations (26/03 afternoon). With this exception, low BC/SO<sub>4</sub> values (< 1), and the chemical composition dominated by ammonium nitrate suggest mid and/or long-range transport.

Episode 6 (28/03/2012 – 31/03/2012): It exhibits the same behaviour than episode 5 with a clear medium-to-long range origin pattern (wind speed ~ 10 km/h, chemical composition dominated by ammonium nitrate), but with backtrajectories coming from NW/NE. Low altitude of backtrajectories illustrate the accumulation of pollutants along the trajectory of the air masses. However, the BC peak on the 30 Mar. morning (the high BC<sub>ff</sub> fraction suggests traffic emissions) could underline an influence of the Paris plume.

Episode 7 (16/01/2013 – 21/01/2013): Air masses display a coiling pattern around Northern France. The BC/SO<sub>4</sub> ratio, remaining lower than 1, suggests advected pollution. However, the strong variability of BC<sub>wb</sub> illustrates a significant influence of wood-burning emissions. No BHL data are available during this episode, but the altitude of backtrajectories may underline a more important dilution of the pollution.

Episode 8 (01/04/2013 – 08/04/2013): This episode actually started in 22/03, but no ACSM data were available at that time; however, meteorological conditions from 22/03 to 01/04 were very similar, notably in terms of wind speeds and direction. It is characterized by air masses originating from the NE and a very low BC/SO<sub>4</sub> ratio, illustrating a typical case of advected secondary pollution, clearly dominated by ammonium nitrate and sulphate.

Overall, the observed variability, in terms of meteorological conditions, air mass origins, and chemical composition illustrates the variety of persistent pollution episodes, in terms of PM sources and different geographical origins. The BC/SO<sub>4</sub> ratio has shown to represent a useful tool to assess the local/regional/advected dimension of a specific pollution episode. Indeed, high ratios ( $\geq 2$ ) are usually associated with accumulation of local and/or regional emissions, while very low ratios ( $\leq 0.5$ ) are more representative of secondary advected pollutants. Ratios within this range should then be associated with a combined influence of regional and advected pollution. Finally, artefact-free ACSM data have shown to be adequate to document semi-volatile aerosols (ammonium nitrate and a fraction of OM), which strongly contribute to PM<sub>1</sub> during persistent pollution episodes, and real-time measurements allow to illustrate the close interactions between the chemical composition and meteorological parameters influencing its temporality.

## 9. Conclusions

Jean-Eudes Petit 15/1/15 23:49

Supprimé: /



The chemical composition of submicron ( $PM_{10}$ ) aerosols was continuously monitored in near real-time at a regional background site of the region of Paris between June 2011 and May 2013 using a combination of an ACSM and an Aethalometer. The obtained 2-year dataset allows an appraisal of the robustness of ACSM measurements over several month periods, as well as Aethalometer measurements and BC source apportionment.

Non-parametric Wind Regression calculations has been performed for each season and provided useful information regarding the geographical origin of  $PM_{10}$  chemical constituents. SIA, in particular ammonium sulphate, show a clear advected pattern, leading to a uniform signal over large scales. Ammonium nitrate also exhibits a significant contribution of regional and local emissions. The highest concentrations of OM were identified as having a major local origin, while regional background OM concentrations remain significant, especially in spring and summer. The region of Brittany (Western France), the major hotspot of ammonia in France, seems to have little influence on the concentrations of this species at our station in the region of Paris; overall regional background concentrations of ammonia dominate, especially in Spring. Similarly to OM, wintertime  $BC_{wb}$  concentrations are mainly from local emissions from domestic heating although a noticeable regional background is still observed for this tracer of wood burning. As expected,  $BC_{ff}$  shows a clear local (nearby) origin, as well as contribution from the Paris city plume, and remains fairly constant throughout seasons, due to its regional traffic origin.

Such near real-time observations over long-term periods offer a unique opportunity to provide robust diurnal profiles for each season. For instance, diurnal profiles of semi-volatile nitrate aerosols were observed in different seasons with temperatures favouring its partitioning into the particulate phase in the morning and in the gas phase in the afternoon. No clear contribution of traffic could be proven regarding ammonia variability, and the regional background seems to prevail.

All the persistent pollution episodes ( $PM_{10} > 20 \mu g/m^3$  during at least 3 consecutive days) which occurred between 2011 and 2013 were carefully examined showing different meteorological conditions, sources and geographical origins making it difficult to draw general rules for these episodes. The  $BC/SO_4$  ratio was used here to better separate local, regional (BC dominated) and advected ( $SO_4$  dominated) contributions, and showed that, with very few exceptions, most of these persistent episodes were dominated by medium-to-long range transported pollution. However, it is interesting to note that the majority of the highest (time-limited)  $PM_{10}$  concentrations (30-min ACSM data points with  $PM_{10} > 50 \mu g/m^3$ ) fell within these persistent pollution episodes and were characterized by a significant local/regional contribution (high  $BC/SO_4$  ratios). This result, obtained with real-time measurements, may offer new perspectives in the definition and the evaluation of the effectiveness of local mitigation policies such as emergency measures (traffic or wood burning restrictions, for instance) taken to improve air quality during pollution events. In parallel, the long-term characterization of the organic fraction would surely lead to a better assessment of aerosol sources and some (trans-)formation processes of secondary pollution in the Ile-de-France area.

Jean-Eudes Petit 15/1/15 23:50

Supprimé: /

Jean-Eudes Petit 15/1/15 23:50

Supprimé: versus



1  
2  
3  
4  
5  
6  
7  
8  
9  
10  
11  
12  
13  
14  
15  
16  
17  
18  
19  
20

In conclusion, these first 2-year quality-controlled measurements of ACSM clearly demonstrate their great potential to monitor on a long term basis aerosol sources and their geographical origin and provide strategic information in near real-time during pollution episodes. They also support the capacity of the ACSM to be proposed as a robust and credible alternative to filter-based sampling techniques for long term monitoring strategies. The networking of such instrumentation (ACSM and BC) throughout Europe – as currently being built up within the European ACTRIS program - will certainly offers tremendous opportunities for modeling studies in order to improve prevision models, as well as large scale spatially and temporally resolved source apportionment studies of organic aerosols using the high potential of ACSM organic fragments.

**Acknowledgments**

The research leading to the these results has received funding from INERIS, CNRS, CEA, the French SOERE-ORAURE network, the European Union Seventh Framework Program (FP7/2007-2013) project ACTRIS under grant agreement n°262254, the DIM-R2DS program for the funding of the ACSM equipment, the PRIMEQUAL-PREQUALIF and ADEME-REBECCA programs for the long term observations of Black Carbon at SIRTa.

## 1    **References**

- 2    Aiken, A. C., Salcedo, D., Cubison, M. J., Huffman, J. A., DeCarlo, P. F., Ulbrich, I. M.,  
3    Docherty, K. S., Sueper, D., Kimmel, J. R., Worsnop, D. R. and others: Mexico City aerosol  
4    analysis during MILAGRO using high resolution aerosol mass spectrometry at the urban  
5    supersite (T0)–Part 1: Fine particle composition and organic source apportionment,  
6    *Atmospheric Chem. Phys.*, 9(17), 6633–6653, 2009.
- 7    Appel, B. R., Tokiwa, Y., Haik, M. and Kothny, E. L.: Artifact particulate sulphate and nitrate  
8    formation on filter media, *Atmos. Environ.*, 18(2), 409–416, 1984.
- 9    Arguez, A. and Vose, R. S.: The Definition of the Standard WMO Climate Normal: The Key  
10    to Deriving Alternative Climate Normals, *Bull. Am. Meteorol. Soc.*, 92(6), 699–704,  
11    doi:10.1175/2010BAMS2955.1, 2011.
- 12    Bari, A., Ferraro, V., Wilson, L. R., Luttinger, D. and Husain, L.: Measurements of gaseous  
13    HONO, HNO<sub>3</sub>, SO<sub>2</sub>, HCl, NH<sub>3</sub>, particulate sulphate and PM<sub>2.5</sub> in New York, NY, *Atmos.*  
14    *Environ.*, 37(20), 2825–2835, doi:10.1016/S1352-2310(03)00199-7, 2003.
- 15    Barmapadimos, I., Keller, J., Oderbolz, D., Hueglin, C. and Prévôt, A. S. H.: One decade of  
16    parallel PM<sub>10</sub> and PM<sub>2.5</sub> measurements in  
17    Europe: trends and variability, *Atmospheric Chem. Phys. Discuss.*, 12(1), 1–43,  
18    doi:10.5194/acpd-12-1-2012, 2012.
- 19    Baum, M. M., Kiyomiya, E. S., Kumar, S., Lappas, A. M., Kapinus, V. A. and Lord, H. C.:  
20    Multicomponent remote sensing of vehicle exhaust by dispersive absorption spectroscopy. 2.  
21    Direct on-road ammonia measurements, *Env. Sci. Technol.*, 35(18), 3735–3741,  
22    doi:10.1021/es002046y, 2001.
- 23    Bond, T. C. and Bergstrom, R. W.: Light Absorption by Carbonaceous Particles: An  
24    Investigative Review, *Aerosol Sci. Technol.*, 40(1), 27–67, doi:10.1080/02786820500421521,  
25    2006.
- 26    Bressi, M., Sciare, J., Gherzi, V., Bonnaire, N., Nicolas, J. B., Petit, J.-E., Moukhtar, S.,  
27    Rosso, A., Mihalopoulos, N. and Féron, A.: A one-year comprehensive chemical  
28    characterisation of fine aerosol (PM<sub>2.5</sub>) at urban, suburban and rural  
29    background sites in the region of Paris (France), *Atmospheric Chem. Phys.*, 13(15), 7825–  
30    7844, doi:10.5194/acp-13-7825-2013, 2013.
- 31    Bussink, D. W., Harper, L. A. and Corré, W. J.: Ammonia Transport in a Temperate  
32    Grassland: II. Diurnal Fluctuations in Response to Weather and Management Conditions,  
33    *Agron J.*, 88(4), 621–626, 1996.
- 34    Cavalli, F., Viana, M., Yttri, K. E., Genberg, J. and Putaud, J.-P.: Toward a standardised  
35    thermal-optical protocol for measuring atmospheric organic and elemental carbon: the  
36    EUSAAR protocol, *Atmospheric Meas. Tech.*, 3, 79–89, doi:10.5194/amt-3-79-2010, 2010.
- 37    Cheng, Y., He, K. B., Duan, F. K., Zheng, M., Ma, Y. L. and Tan, J. H.: Positive sampling

1 artifact of carbonaceous aerosols and its influence on the thermal-optical split of OC/EC,  
2 Atmospheric Chem. Phys., 9(18), 7243–7256, 2009.

3 Chow, J. C., Watson, J. G., Mauderly, J. L., Costa, D. L., Wyzga, R. E., Vedal, S., Hidy, G.  
4 M., Altshuler, S. L., Marrack, D., Heuss, J. M., Wolff, G. T., Pope, C. A. and Dockery, D.  
5 W.: Health Effects of Fine Particulate Air Pollution: Lines that Connect, J. Air Waste Manag.  
6 Assoc., 56, 1368–1380, 2006.

7 Collaud Coen, M., Weingartner, E., Apituley, A., Ceburnis, D., Fierz-Schmidhauser, R.,  
8 Flentje, H., Henzing, J. S., Jennings, S. G., Moerman, M. and Petzold, A.: Minimizing light  
9 absorption measurement artifacts of the Aethalometer: evaluation of five correction  
10 algorithms, Atmospheric Meas. Tech., 3, 457–474, 2010.

11 Cowen, K., Sumner, A. L., Dinhal, A., Riggs, K. and Willenberg, Z.: Environmental  
12 Technology Verification Report, Mechatronics Instruments BV AiRRmonia Ammonia  
13 Analyzer., 2004.

14 Crippa, M., Canonaco, F., Slowik, J. G., El Haddad, I., DeCarlo, P. F., Mohr, C., Heringa, M.  
15 F., Chirico, R., Marchand, N., Temime-Roussel, B., Abidi, E., Poulain, L., Wiedensohler, A.,  
16 Baltensperger, U. and Prevot, A. S. H.: Primary and secondary organic aerosol origin by  
17 combined gas-particle phase source apportionment, Atmos Chem Phys Discuss, 13, 8537–  
18 8583, 2013a.

19 Crippa, M., DeCarlo, P. F., Slowik, J. G., Mohr, C., Heringa, M. F., Chirico, R., Poulain, L.,  
20 Freutel, F., Sciare, J., Cozic, J., Di Marco, C. F., Elsasser, M., Nicolas, J. B., Marchand, N.,  
21 Abidi, E., Wiedensohler, A., Drewnick, F., Schneider, J., Borrmann, S., Nemitz, E.,  
22 Zimmermann, R., Jaffrezou, J.-L., Prévôt, A. S. H. and Baltensperger, U.: Wintertime aerosol  
23 chemical composition and source apportionment of the organic fraction in the metropolitan  
24 area of Paris, Atmospheric Chem. Phys., 13(2), 961–981, doi:10.5194/acp-13-961-2013,  
25 2013b.

26 Dall’Osto, M., Ovadnevaite, J., Ceburnis, D., Martin, D., Healy, R. M., O’Connor, I. P.,  
27 Kourtchev, I., Sodeau, J. R., Wenger, J. C. and O’Dowd, C.: Characterization of urban aerosol  
28 in Cork city (Ireland) using aerosol mass spectrometry, Atmospheric Chem. Phys., 13(9),  
29 4997–5015, doi:10.5194/acp-13-4997-2013, 2013.

30 Draxler, R.: Hysplit4 User’s Guide. [online] Available from:  
31 <http://www.arl.noaa.gov/documents/reports/arl-230.pdf> (Accessed 14 May 2014), 1999.

32 [Drinovec, L., Mocnik, G., Zotter, P., Prevot, A. S. H., Ruckstuhl, C., Coz Diego, E.,](#)  
33 [Rupakheti, M., Sciare, J., Mueller, T., Wiedensohler, A. T. and Hansen, A. D. A.: The “Dual-](#)  
34 [Spot” Aethalometer: improved measurement of Aerosol Black Carbon with real-time loading](#)  
35 [compensation, Atmos Meas Tech Discuss, 2014.](#)

36 Edgerton, E. S., Saylor, R. D., Hartsell, B. E., Jansen, J. J. and Alan Hansen, D.: Ammonia  
37 and ammonium measurements from the southeastern United States, Atmos. Environ., 41(16),  
38 3339–3351, doi:10.1016/j.atmosenv.2006.12.034, 2007.

1 Favez, O., Cachier, H., Sciare, J., Sarda-estève, R. and Martinon, L.: Evidence for a  
2 significant contribution of wood burning aerosols to PM<sub>2.5</sub> during the winter season in Paris,  
3 France, *Atmos. Environ.*, 43, 3640–3644, 2009.

4 Favez, O., El Haddad, I., Piot, C., Boréave, A., Abidi, E., Marchand, N., Jaffrezo, J. L.,  
5 Besombes, J. L., Personnaz, M. B., Sciare, J., Wortham, H., George, C. and D’anna, B.: Inter-  
6 comparison of source apportionment models for the estimation of wood burning aerosols  
7 during wintertime in an Alpine city (Grenoble, France), *Atmos Chem Phys*, 10, 5295–5314,  
8 doi:10.5194/acp-10-5295-2010, 2010.

9 Freutel, F., Schneider, J., Drewnick, F., von der Weiden-Reinmüller, S.-L., Crippa, M.,  
10 Prévôt, A. S. H., Baltensperger, U., Poulain, L., Wiedensohler, A., Sciare, J., Sarda-Estève,  
11 R., Burkhardt, J. F., Eckhardt, S., Stohl, A., Gros, V., Colomb, A., Michoud, V., Doussin, J. F.,  
12 Borbon, A., Haeffelin, M., Morille, Y., Beekmann, M. and Borrmann, S.: Aerosol particle  
13 measurements at three stationary sites in the megacity of Paris during summer 2009:  
14 meteorology and air mass origin dominate aerosol particle composition and size distribution,  
15 *Atmospheric Chem. Phys.*, 13(2), 933–959, doi:10.5194/acp-13-933-2013, 2013.

16 Fröhlich, R., Crenn, V., Setyan, A., Belis, C. A., Canonaco, F., Favez, O., Riffault, V.,  
17 Slowik, J. G., Aas, W., Aijälä, M., Alastuey, A., Artiñano, B., Bonnaire, N., Bozzetti, C.,  
18 Bressi, M., Carbone, C., Coz, E., Croteau, P. L., Cubison, M. J., Esser-Gietl, J. K., Green, D.  
19 C., Gros, V., Heikkinen, L., Herrmann, H., Jayne, J. T., Lunder, C. R., Minguillón, M. C.,  
20 Močnik, G., O’Dowd, C. D., Ovadnevaite, J., Petralia, E., Poulain, L., Priestman, M., Ripoll,  
21 A., Sarda-Estève, R., Wiedensohler, A., Baltensperger, U., Sciare, J. and Prévôt, A. S. H.:  
22 ACTRIS ACSM intercomparison – Part 2: Intercomparison of ME-2 organic source  
23 apportionment results from 15 individual, co-located aerosol mass spectrometers,  
24 Atmospheric Meas. Tech. Discuss., 8(2), 1559–1613, doi:10.5194/amtd-8-1559-2015, 2015.

25 Grover, B. D.: Measurement of total PM<sub>2.5</sub> mass (nonvolatile plus semivolatile) with the  
26 Filter Dynamic Measurement System tapered element oscillating microbalance monitor, *J.*  
27 *Geophys. Res.*, 110(D7), doi:10.1029/2004JD004995, 2005.

28 Haeffelin, M., Barthès, L., Bock, O., Boitel, C., Bony, S., Bouniol, D., Chepfer, H., Chiriaco,  
29 M., Cuesta, J. and Delanoë, J.: SIRTa, a ground-based atmospheric observatory for cloud and  
30 aerosol research, *Ann. Geophys.*, 253–275, 2005.

31 Henry, R., Norris, G. A., Vedantham, R. and Turner, J. R.: Source Region Identification  
32 Using Kernel Smoothing, *Environ. Sci. Technol.*, 43(11), 4090–4097,  
33 doi:10.1021/es8011723, 2009.

34 IARC: Outdoor air pollution a leading environmental cause of cancer deaths, press release  
35 n°221,, 2013.

36 Janssen, N. A., Hoek, G., Simic-Lawson, M., Fischer, P., van Bree, L., ten Brink, H., Keuken,  
37 M., Atkinson, R. W., Anderson, H. R., Brunekreef, B. and others: Black carbon as an  
38 additional indicator of the adverse health effects of airborne particles compared with PM<sub>10</sub>  
39 and PM<sub>2.5</sub>, *Env. Health Perspect.*, 119(12), 1691–1699, 2011.

Jean-Eudes Petit 18/2/15 10:18

Mis en forme: Police :(Par défaut) Times  
New Roman

1 Jayne, J. T., Leard, D. C., Zhang, X., Davidovits, P., Smith, K. S., Kolb, C. E. and Worsnop,  
2 D. R.: Development of an Aerosol Mass Spectrometer for Size and Composition Analysis of  
3 Submicron Particles, *Aerosol Sci. Technol.*, 33, 49–70, 2000.

4 Jimenez, J. L., Canagaratna, M. R., Donahue, N. M., Prevot, A. S. H., Zhang, Q., Kroll, J. H.,  
5 DeCarlo, P. F., Allan, J. D., Coe, H., Ng, N. L., Aiken, A. C., Docherty, K. S., Ulbrich, I. M.,  
6 Grieshop, A. P., Robinson, A. L., Duplissy, J., Smith, J. D., Wilson, K. R., Lanz, V. A.,  
7 Hueglin, C., Sun, Y. L., Tian, J., Laaksonen, A., Raatikainen, T., Rautiainen, J., Vaattovaara,  
8 P., Ehn, M., Kulmala, M., Tomlinson, J. M., Collins, D. R., Cubison, M. J., Dunlea, E. J.,  
9 Huffman, J. A., Onasch, T. B., Alfarra, M. R., Williams, P. I., Bower, K., Kondo, Y.,  
10 Schneider, J., Drewnick, F., Borrmann, S., Weimer, S., Demerjian, K., Salcedo, D., Cottrell,  
11 L., Griffin, R., Takami, A., Miyoshi, T., Hatakeyama, S., Shimono, A., Sun, J. Y., Zhang, Y.  
12 M., Dzepina, K., Kimmel, J. R., Sueper, D., Jayne, J. T., Herndon, S. C., Trimborn, A. M.,  
13 Williams, L. R., Wood, E. C., Middlebrook, A. M., Kolb, C. E., Baltensperger, U. and  
14 Worsnop, D. R.: Evolution of Organic Aerosols in the Atmosphere, *Science*, 326(5959),  
15 1525–1529, doi:10.1126/science.1180353, 2009.

16 Kai, Z., Yuesi, W., Tianxue, W., Yousef, M. and Frank, M.: Properties of nitrate, sulphate and  
17 ammonium in typical polluted atmospheric aerosols (PM10) in Beijing, *Atmospheric Res.*,  
18 84(1), 67–77, doi:10.1016/j.atmosres.2006.05.004, 2007.

19 Lack, D. A., Cappa, C. D., Covert, D. S., Baynard, T., Massoli, P., Sierau, B., Bates, T. S.,  
20 Quinn, P. K., Lovejoy, E. R. and Ravishankara, A. R.: Bias in Filter-Based Aerosol Light  
21 Absorption Measurements Due to Organic Aerosol Loading: Evidence from Ambient  
22 Measurements, *Aerosol Sci. Technol.*, 42(12), 1033–1041, doi:10.1080/02786820802389277,  
23 2008.

24 Lin, Y., Cheng, M., Ting, W. and Yeh, C.: Characteristics of gaseous HNO<sub>2</sub>, HNO<sub>3</sub>, NH<sub>3</sub>  
25 and particulate ammonium nitrate in an urban city of Central Taiwan, *Atmos. Environ.*,  
26 40(25), 4725–4733, doi:10.1016/j.atmosenv.2006.04.037, 2006.

27 Middlebrook, A. M., Bahreini, R., Jimenez, J. L. and Canagaratna, M. R.: Evaluation of  
28 Composition-Dependent Collection Efficiencies for the Aerodyne Aerosol Mass Spectrometer  
29 using Field Data, *Aerosol Sci. Technol.*, 46(3), 258–271,  
30 doi:10.1080/02786826.2011.620041, 2012.

31 Ng, N. L., Herndon, S. C., Trimborn, A., Canagaratna, M. R., Croteau, P. L., Onasch, T. B.,  
32 Sueper, D., Worsnop, D. R., Zhang, Q. and Sun, Y. L.: An aerosol chemical speciation  
33 monitor (ACSM) for routine monitoring of the composition and mass concentrations of  
34 ambient aerosol, *Aerosol Sci. Technol.*, 45(7), 780–794, 2011.

35 Nussbaumer, T., Czasch, C., Klippel, N., Johansson, L. and Tullin, C.: Particulate emissions  
36 from biomass combustion in IEA countries, [online] Available from: [http://www.vbt.uni-](http://www.vbt.uni-karlsruhe.de/index.pl/themen/mahe_wirbel/literatur/Wood-Single-Aspects/Emissions/Partikulate-Emissions-from-Biomass-Combustion-in-IEA-Countries_Nussbaumer_IEA_2008.pdf)  
37 [karlsruhe.de/index.pl/themen/mahe\\_wirbel/literatur/Wood-Single-](http://www.vbt.uni-karlsruhe.de/index.pl/themen/mahe_wirbel/literatur/Wood-Single-Aspects/Emissions/Partikulate-Emissions-from-Biomass-Combustion-in-IEA-Countries_Nussbaumer_IEA_2008.pdf)  
38 [Aspects/Emissions/Partikulate-Emissions-from-Biomass-Combustion-in-IEA-](http://www.vbt.uni-karlsruhe.de/index.pl/themen/mahe_wirbel/literatur/Wood-Single-Aspects/Emissions/Partikulate-Emissions-from-Biomass-Combustion-in-IEA-Countries_Nussbaumer_IEA_2008.pdf)  
39 [Countries\\_Nussbaumer\\_IEA\\_2008.pdf](http://www.vbt.uni-karlsruhe.de/index.pl/themen/mahe_wirbel/literatur/Wood-Single-Aspects/Emissions/Partikulate-Emissions-from-Biomass-Combustion-in-IEA-Countries_Nussbaumer_IEA_2008.pdf) (Accessed 11 June 2014), 2008.

- 1 Olson, D. A., Vedantham, R., Norris, G. A., Brown, S. G. and Roberts, P.: Determining  
2 source impacts near roadways using wind regression and organic source markers, *Atmos.*  
3 *Environ.*, 47, 261–268, doi:10.1016/j.atmosenv.2011.11.003, 2012.
- 4 [Pal, S., Haeffelin, M. and Batchvarova, E.: Exploring a geophysical process-based attribution  
5 technique for the determination of the atmospheric boundary layer depth using aerosol lidar  
6 and near-surface meteorological measurements: NEW ATTRIBUTION LIDAR-DERIVED  
7 ABL DEPTH, \*J. Geophys. Res. Atmospheres\*, 118\(16\), 9277–9295, doi:10.1002/jgrd.50710,  
8 2013.](#)
- 9 Pancras, J. P., Vedantham, R., Landis, M. S., Norris, G. A. and Ondov, J. M.: Application of  
10 EPA Unmix and Nonparametric Wind Regression on High Time Resolution Trace Elements  
11 and Speciated Mercury in Tampa, Florida Aerosol, *Environ. Sci. Technol.*, 45(8), 3511–3518,  
12 doi:10.1021/es103400h, 2011.
- 13 Pandolfi, M., Amato, F., Reche, C., Alastuey, A., Otjes, R. P., Blom, M. J. and Querol, X.:  
14 Summer ammonia measurements in a densely populated Mediterranean city, *Atmospheric*  
15 *Chem. Phys.*, 12(16), 7557–7575, doi:10.5194/acp-12-7557-2012, 2012.
- 16 Pathak, R., Yao, X. and Chan, C.: Sampling artifacts of acidity and ionic species in PM<sub>2.5</sub>,  
17 *Environ. Sci. Technol.*, 38(1), 254–259, doi:10.1021/es0342244, 2004.
- 18 Petit, J.-E., Favez, O., Sciare, J., Canonaco, F., Croteau, P., Močnik, G., Jayne, J., Worsnop,  
19 D. and Leoz-Garziandia, E.: Submicron aerosol source apportionment of wintertime pollution  
20 in Paris, France by Double Positive Matrix Factorization (PMF<sup>2</sup>)<br>21 using Aerosol Chemical Speciation Monitor (ACSM) and multi-wavelength Aethalometer,  
22 *Atmospheric Chem. Phys. Discuss.*, 14(10), 14159–14199, doi:10.5194/acpd-14-14159-2014,  
23 2014.
- 24 Pope, C. A. and Dockery, D. W.: Health Effects of Fine Particulate Air Pollution: Lines that  
25 Connect, *J. Air Waste Manag. Assoc.*, 56(6), 709–742,  
26 doi:10.1080/10473289.2006.10464485, 2006.
- 27 Putaud, J.-P., Raes, F., Van Dingenen, R., Brüggemann, E., Facchini, M.-C., Decesari, S.,  
28 Fuzzi, S., Gehrig, R., Hüglin, C., Laj, P., Lorbeer, G., Maenhaut, W., Mihalopoulos, N.,  
29 Müller, K., Querol, X., Rodriguez, S., Schneider, J., Spindler, G., Brink, H. ten, Tørseth, K.  
30 and Wiedensohler, A.: A European aerosol phenomenology—2: chemical characteristics of  
31 particulate matter at kerbside, urban, rural and background sites in Europe, *Atmos. Environ.*,  
32 38(16), 2579–2595, doi:10.1016/j.atmosenv.2004.01.041, 2004.
- 33 Ramgolam, K., Favez, O., Cachier, H., Gaudichet, A., Marano, F., Martinon, L. and Baeza-  
34 Squiban, A.: Size-partitioning of an urban aerosol to identify particle determinants involved in  
35 the proinflammatory response induced in airway epithelial cells, *Part. Fibre Toxicol.*, 6(10),  
36 doi:10.1186/1743-8977-6-10, 2009.
- 37 Rengarajan, R., Sudheer, A. K. and Sarin, M. M.: Wintertime PM<sub>2.5</sub> and PM<sub>10</sub> carbonaceous  
38 and inorganic constituents from urban site in western India, *Atmospheric Res.*, 102(4), 420–  
39 431, doi:10.1016/j.atmosres.2011.09.005, 2011.

Jean-Eudes Petit 18/2/15 10:18

Mis en forme: Police :(Par défaut) Times  
New Roman

1 Sandradewi, J., Prévôt, A. S. H., Szidat, S., Perron, N., Alfarra, M. R., Lanz, V. A.,  
2 Weingartner, E. and Baltensperger, U.: Using Aerosol Light Absorption Measurements for  
3 the Quantitative Determination of Wood Burning and Traffic Emission Contributions to  
4 Particulate Matter, *Environ. Sci. Technol.*, 42(9), 3316–3323, doi:10.1021/es702253m, 2008.

5 Saylor, R. D., Edgerton, E. S., Hartsell, B. E., Baumann, K. and Hansen, D. A.: Continuous  
6 gaseous and total ammonia measurements from the southeastern aerosol research and  
7 characterization (SEARCH) study, *Atmos. Environ.*, 44(38), 4994–5004,  
8 doi:10.1016/j.atmosenv.2010.07.055, 2010.

9 Sciare, J., d' Argouges, O., Sarda-Estève, R., Gaimoz, C., Dolgorouky, C., Bonnaire, N.,  
10 Favez, O., Bonsang, B. and Gros, V.: Large contribution of water-insoluble secondary organic  
11 aerosols in the region of Paris (France) during wintertime, *J. Geophys. Res. Atmospheres*,  
12 116(D22), n/a–n/a, doi:10.1029/2011JD015756, 2011.

13 Sciare, J., d' Argouges, O., Zhang, Q. J., Sarda-Estève, R., Gaimoz, C., Gros, V., Beekmann,  
14 M. and Sanchez, O.: Comparison between simulated and observed chemical composition of  
15 fine aerosols in Paris (France) during springtime: contribution of regional versus continental  
16 emissions, *Atmospheric Chem. Phys.*, 10(24), 11987–12004, doi:10.5194/acp-10-11987-  
17 2010, 2010.

18 Sciare, J., Sarda-estève, R., Favez, O., Cachier, H., Aymoz, G. and Laj, P.: Nighttime  
19 residential wood burning evidenced from an indirect method for estimating real-time  
20 concentration of particulate organic matter (POM), *Atmos. Environ.*, 42, 2158–2172, 2008.

21 Takegawa, N., Miyazaki, Y., Kondo, Y., Komazaki, Y., Miyakawa, T., Jimenez, J. L., Jayne,  
22 J. T., Worsnop, D. R., Allan, J. D. and Weber, R. J.: Characterization of an Aerodyne Aerosol  
23 Mass Spectrometer (AMS): Intercomparison with Other Aerosol Instruments, *Aerosol Sci.*  
24 *Technol.*, 39(8), 760–770, doi:10.1080/02786820500243404, 2005.

25 Turpin, B. J., Huntzicker, J. J. and Hering, S. V.: Investigation of organic aerosol sampling  
26 artifacts in the Los Angeles Basin, *Atmos. Environ.*, 28(19), 3061–3071, 1994.

27 Waked, A., Favez, O., Alleman, L. Y., Piot, C., Petit, J.-E., Delaunay, T., Verlinden, E.,  
28 Golly, B., Besombes, J.-L., Jaffrezo, J.-L. and Leoz-Garziandia, E.: Source apportionment of  
29 PM<sub>10</sub> in a north-western Europe regional urban background site  
30 (Lens, France) using positive matrix factorization and including primary biogenic emissions,  
31 *Atmospheric Chem. Phys.*, 14(7), 3325–3346, doi:10.5194/acp-14-3325-2014, 2014.

32 Weingartner, E., Saathoff, H., Schnaiter, M., Streit, N., Bitnar, B. and Baltensperger, U.:  
33 Absorption of light by soot particles: determination of the absorption coefficient by means of  
34 aethalometers, *J. Aerosol Sci.*, 34, 1445–1463, 2003.

35 Yiou, P. and Cattiaux, J.: Contribution of Atmospheric circulation to wet North European  
36 summer precipitation of 2012, *Am. Meteorol. Soc.* [online] Available from:  
37 [http://docs.house.gov/meetings/IF/IF03/20130918/101308/HHRG-113-IF03-20130918-](http://docs.house.gov/meetings/IF/IF03/20130918/101308/HHRG-113-IF03-20130918-SD011.pdf)  
38 [SD011.pdf](http://docs.house.gov/meetings/IF/IF03/20130918/101308/HHRG-113-IF03-20130918-SD011.pdf) (Accessed 14 May 2014), 2013.

1 Yu, K. ., Cheung, Y. ., Cheung, T. and Henry, R. C.: Identifying the impact of large urban  
2 airports on local air quality by nonparametric regression, *Atmos. Environ.*, 38(27), 4501–  
3 4507, doi:10.1016/j.atmosenv.2004.05.034, 2004.

4 Zechmeister-Boltenstern, S.: Training on NH<sub>3</sub> measurement by wet chemistry techniques,  
5 ACTRIS TNA Activity Report., 2010.

6 Zhang, Q., Jimenez, J. L., Canagaratna, M. R., Allan, J. D., Coe, H., Ulbrich, I., Alfarra, M.  
7 R., Takami, A., Middlebrook, A. M., Sun, Y. L., Dzepina, K., Dunlea, E., Docherty, K.,  
8 DeCarlo, P. F., Salcedo, D., Onasch, T., Jayne, J. T., Miyoshi, T., Shimo, A., Hatakeyama,  
9 S., Takegawa, N., Kondo, Y., Schneider, J., Drewnick, F., Borrmann, S., Weimer, S.,  
10 Demerjian, K., Williams, P., Bower, K., Bahreini, R., Cottrell, L., Griffin, R. J., Rautiainen,  
11 J., Sun, J. Y., Zhang, Y. M. and Worsnop, D. R.: Ubiquity and dominance of oxygenated  
12 species in organic aerosols in anthropogenically-influenced Northern Hemisphere  
13 midlatitudes, *Geophys. Res. Lett.*, 34(13), doi:10.1029/2007GL029979, 2007.

14 Zhang, Q., Stanier, C. O., Canagaratna, M. R., Jayne, J. T., Worsnop, D. R., Pandis, S. N. and  
15 Jimenez, J. L.: Insights into the Chemistry of New Particle Formation and Growth Events in  
16 Pittsburgh Based on Aerosol Mass Spectrometry, *Environ. Sci. Technol.*, 38(18), 4797–4809,  
17 doi:10.1021/es035417u, 2004.

18

19

20

21



1    Table 1. Response factors obtained through IE calibrations from June 2011 to May 2013

<u>Date</u>	<u>Response Factor</u>	<u>RIE<sub>NH4</sub></u>	<u>RIE<sub>SO4</sub></u>
<u>16/11/2011</u>	<u>2.31 10<sup>-11</sup></u>	<u>6</u>	<u>-</u>
<u>09/10/2012</u>	<u>2.98 10<sup>-11</sup></u>	<u>4.8</u>	<u>-</u>
<u>15/05/2013</u>	<u>2.84 10<sup>-11</sup></u>	<u>6.84</u>	<u>1.25</u>
<b><u>Average</u></b>	<b><u>2.72 10<sup>-11</sup></u></b>	<b><u>5.88</u></b>	<b><u>-</u></b>
<b><u>Standard deviation</u></b>	<b><u>13%</u></b>	<b><u>17%</u></b>	<b><u>-</u></b>

2  
3  
4  
5

1 | Table 2. Essential parameters describing the 8 pollution episodes, such as the start and end date, average temperature and relative humidity,  
 2 | fraction dominating the chemical composition (SIA stands for Secondary Inorganic Aerosols), BC-to-SO<sub>4</sub> ratio and main geographical  
 3 | contribution

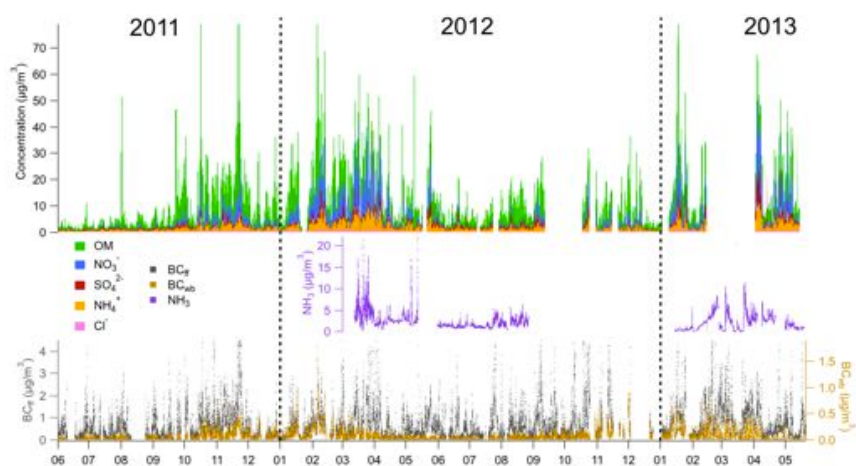
Episode #	Start –end date	Temp. (°C)	RH (%)	Chemical Composition	BC/SO <sub>4</sub>	Geographical contribution
1	19/11/2011 - 24/11/2011	8.5	93	OM	3.56	Regional
2	05/02/2012 - 13/02/2012	-4.7	71	OM then SIA	0.91	Strong local, then regional and advected
3	29/02/2012 - 03/03/2012	8.2	95	SIA	1.12	Strong regional, low advected
4	12/03/2012 - 17/03/2012	10.7	78	SIA	0.95	Advected and regional
5	23/03/2012 - 26/03/2012	15	48	SIA	2.37	Strong advected, low regional
6	28/03/2012 - 31/03/2012	12.3	62	SIA	1.42	Strong advected and regional
7	16/01/2012 - 21/01/2012	-3	93	OM & SIA	0.72	Strong regional and advected
8	01/04/2013 - 08/04/2013	4.2	64	SIA	0.12	Advected

4

Jean-Eudes Petit 6/11/14 11:50

Supprimé: 1

1



2

3 Figure 1: Time series of the major 30-min non-refractory (top, concentrations are aggregated)  
 4 and 5-min refractory (bottom, concentrations are dissociated) PM<sub>1</sub> chemical constituents, and  
 5 5-min ammonia at SIRTa from June 2011 to May 2013. The two large data gaps in October  
 6 2012 and March 2013 correspond to two field intensive campaigns during which the ACSM  
 7 was deployed elsewhere.

8

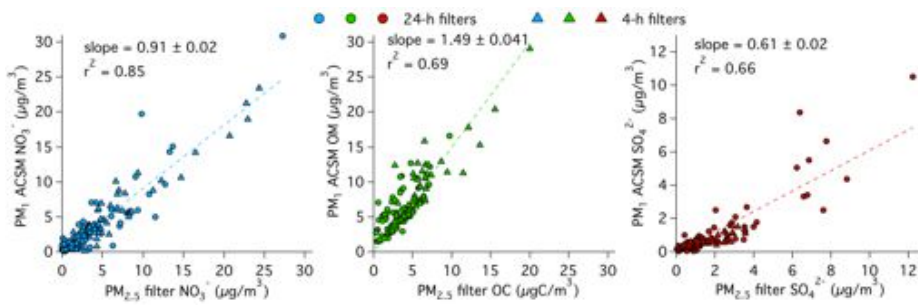
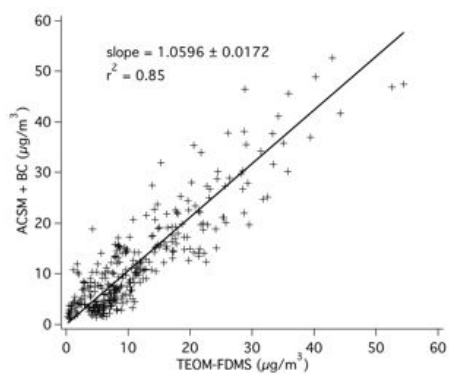


Figure 2: Scatter plot of chemically-speciated ACSM measurements versus filter analyses for nitrate, organic matter (compared to OC filter-based measurements) and sulphate.



1

2 Figure 3: Mass closure exercise between daily averaged reconstructed PM<sub>1</sub> (ACSM + BC)  
 3 and measured PM<sub>1</sub> by TEOM-FDMS.

4

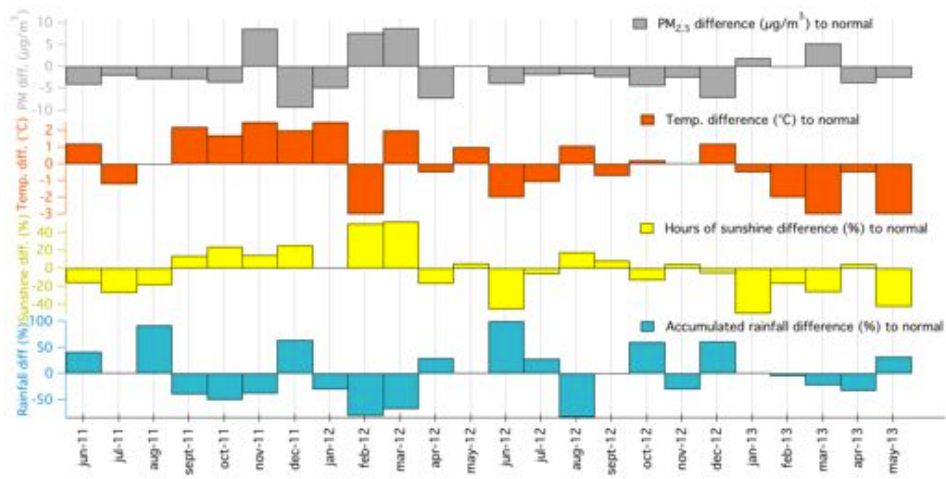


Figure 4: Comparison between observed and average PM<sub>2.5</sub>, temperature, hours of sunshine and accumulated rainfall in the region of Paris.

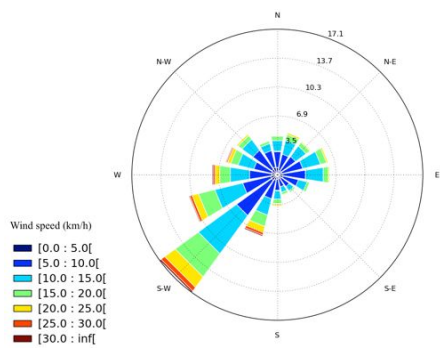


Figure 5: Average wind rose during Jun. 2011 and Jun. 2013, the radial axis represents the wind occurrence (in %).

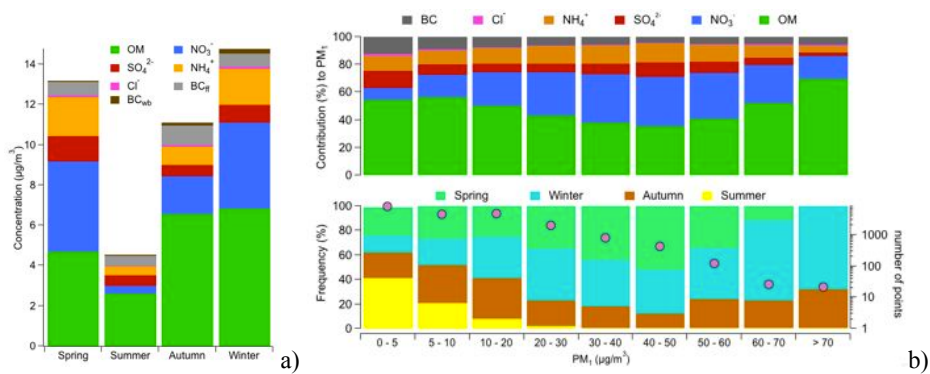


Figure 6: a) PM<sub>1</sub> chemical composition for different mass classes (top), with the seasonal occurrence frequency and number of points in each bin (bottom) b) seasonal PM<sub>1</sub> chemical composition.

Jean-Eudes Petit 27/1/15 16:22

**Supprimé:** Each data point correspond to 1 ACSM (30-min) measurement



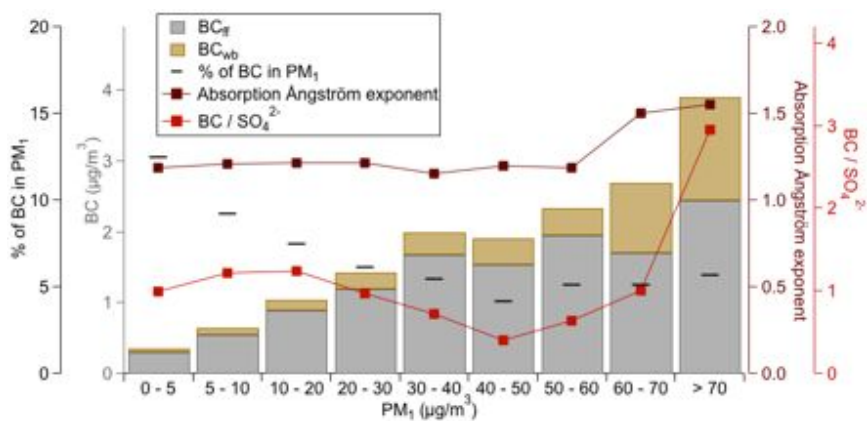
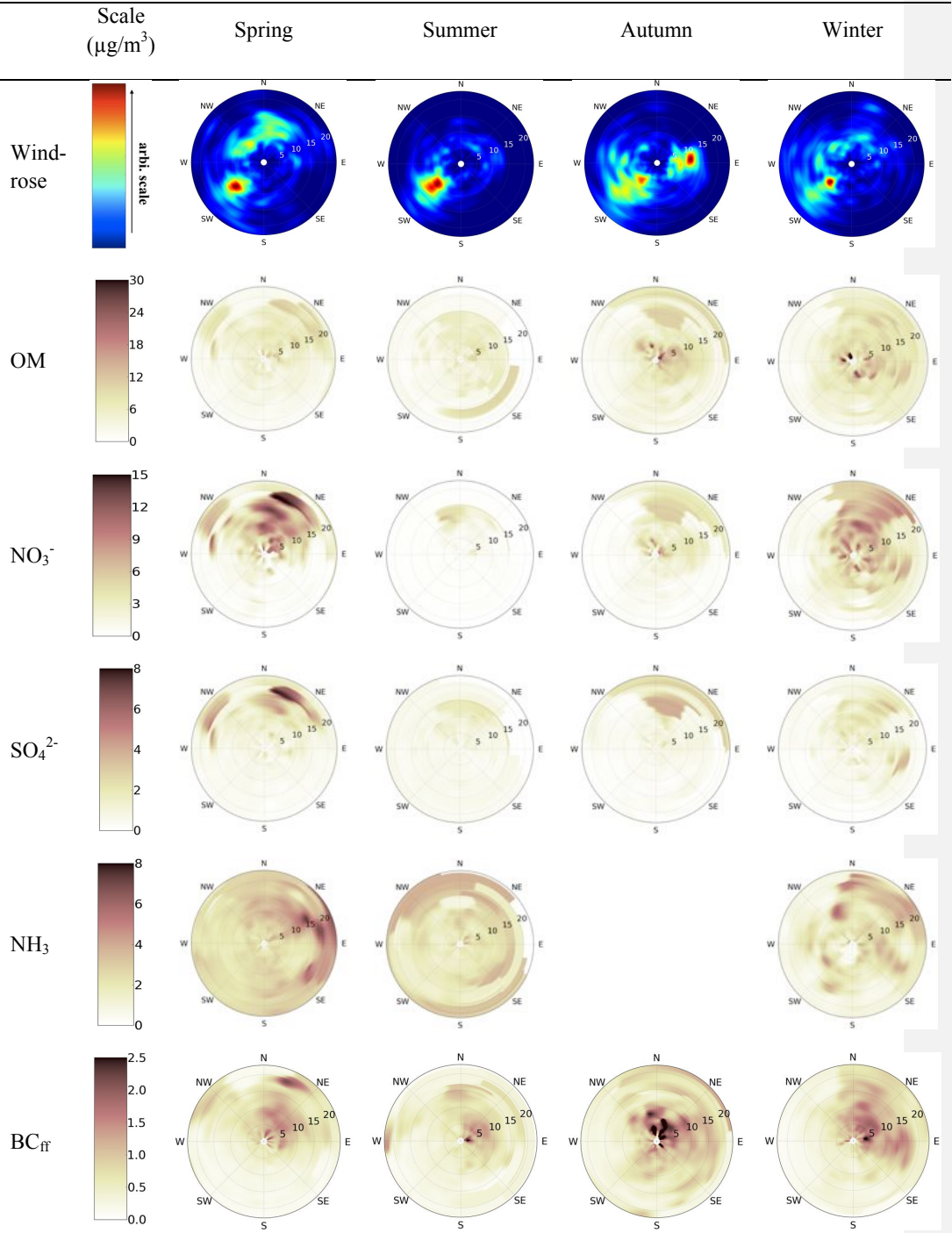
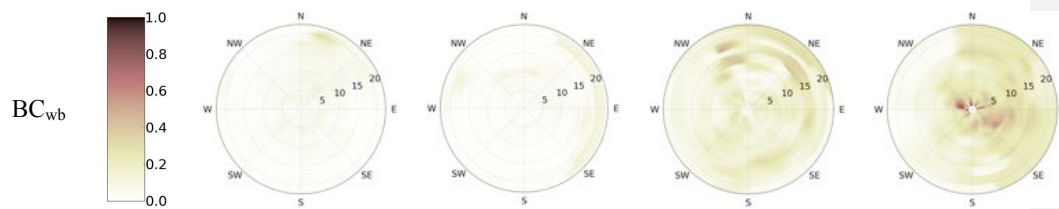


Figure 7: Source contribution to BC, absorption Ångström exponent, BC-SO<sub>4</sub> ratio (ACSM sulphate), and contribution of BC to PM<sub>1</sub>, depending on PM<sub>1</sub> mass.





- 1 Figure 8: Seasonal NWR plots for the major components of  $PM_{10}$  and gaseous ammonia.
- 2 Radial and tangential axes represent the wind direction and speed (km/h), respectively.
- 3

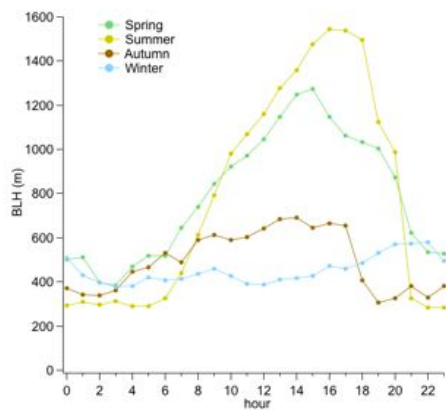
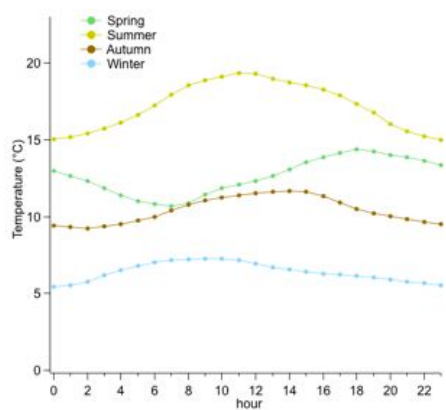
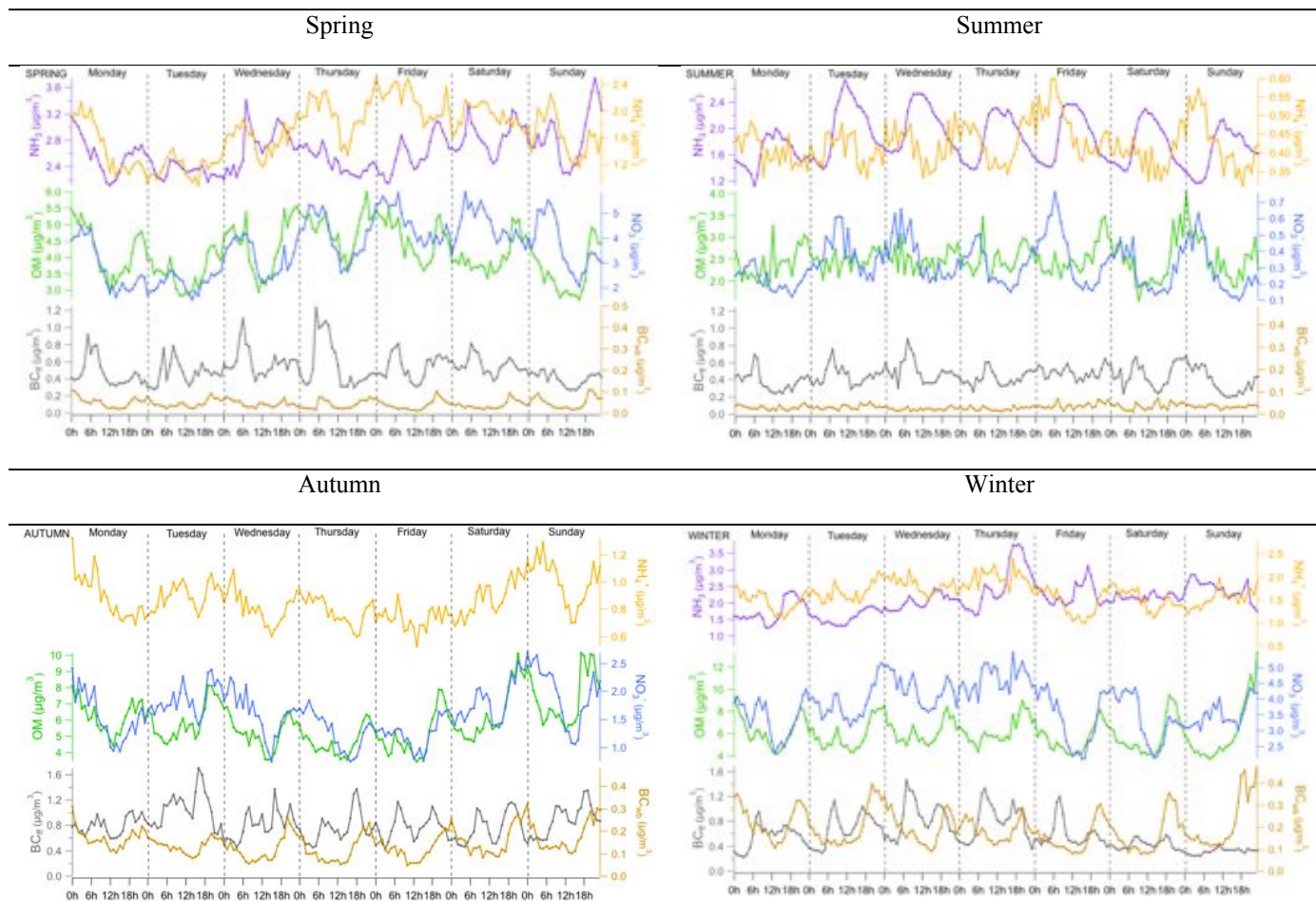


Figure 9: Average diurnal variations by seasons of temperature (a) and BLH (b)



1 Figure 10: Seasonal weekly diurnal variations of OM (green),  $\text{NO}_3^-$  (blue),  $\text{NH}_4^+$  (dark yellow),  $\text{NH}_3$  (purple),  $\text{BC}_{\text{ff}}$  (black) and  $\text{BC}_{\text{wb}}$  (brown)

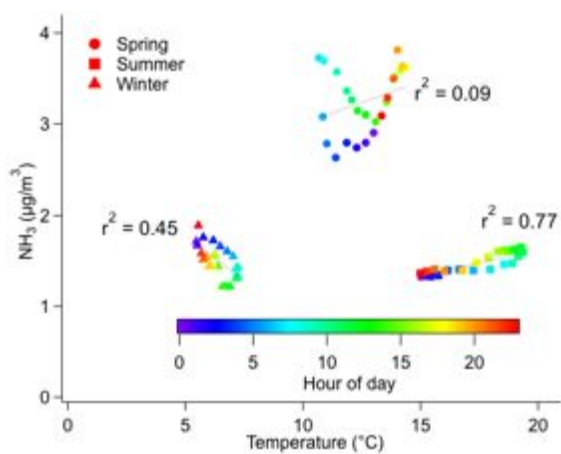
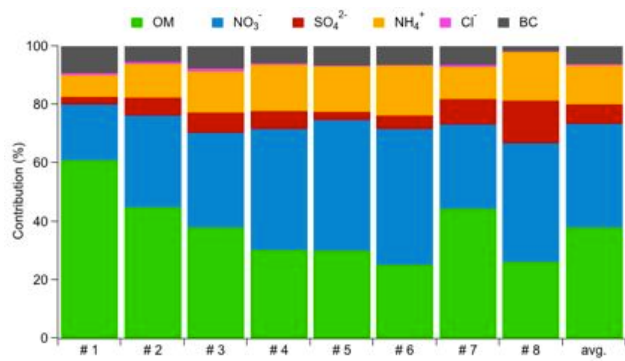


Figure 11: Correlation between ammonia and temperature in Spring (circles), Summer (squares) and Winter (triangles) coloured as a function of the hour of day.

1

2

3    Figure 12: PM<sub>1</sub> chemical composition of the 8 pollution episodes

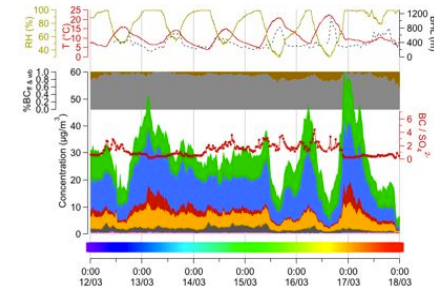
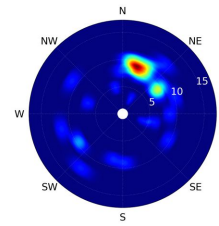
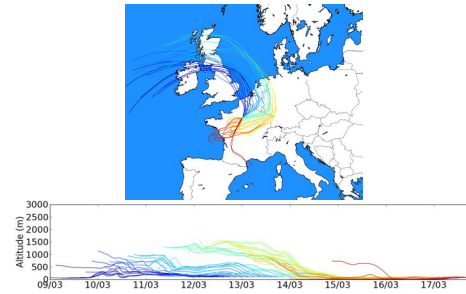






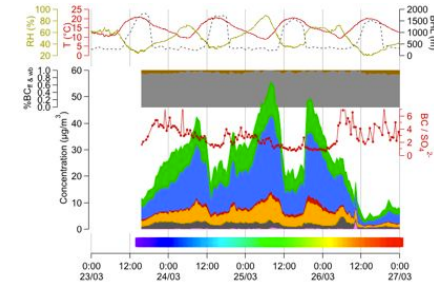
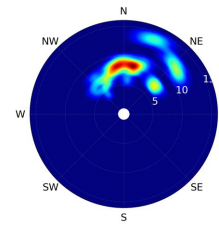
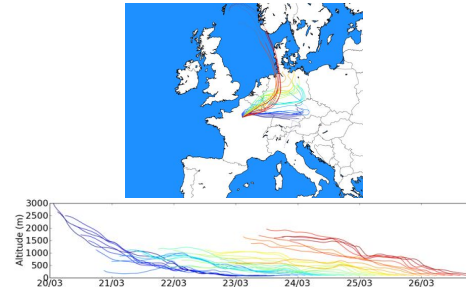
#4  
12/03/2012 – 18/03/2012

0.95



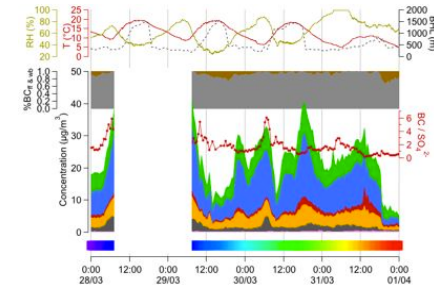
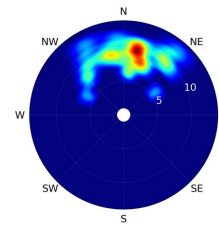
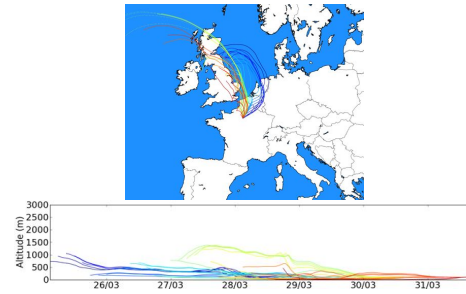
#5  
23/03/2012 – 26/03/2012

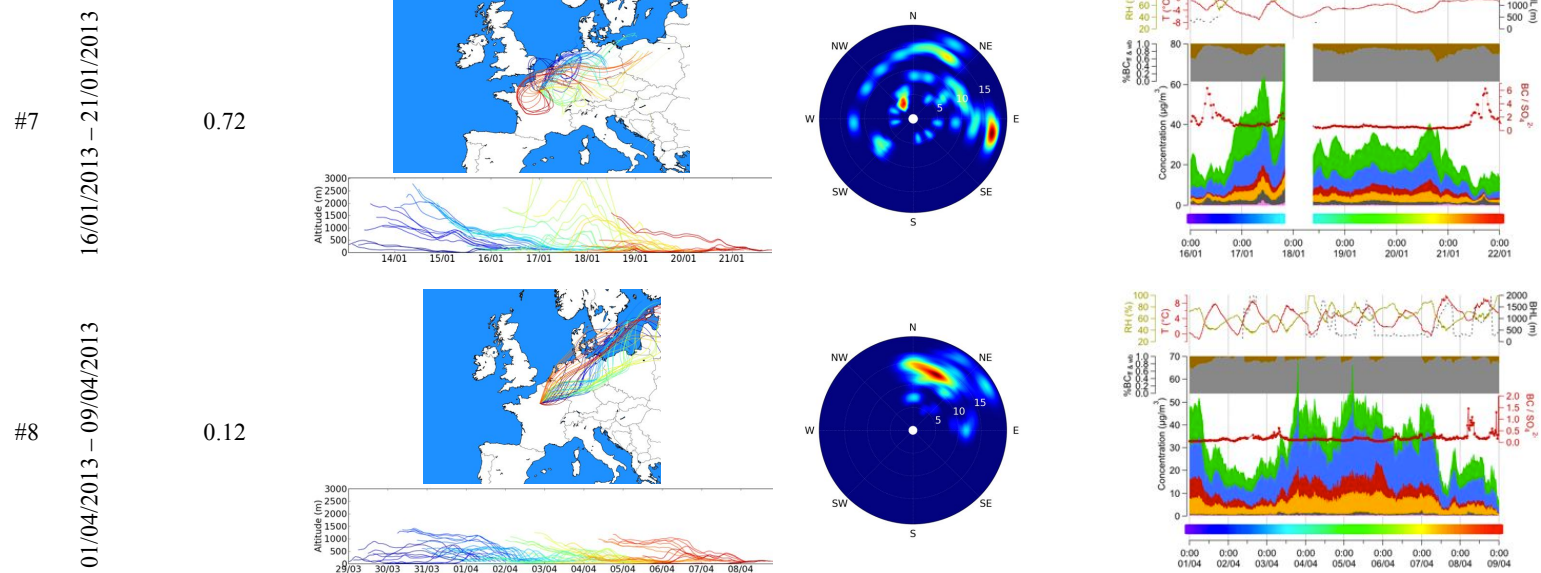
2.37



#6  
28/03/2012 – 01/04/2012

1.42





1 Figure 13: Illustration of meteorological conditions and chemical composition during the 8 pollution episodes. Left graphs represent 72h-backtrajectories  
2 ending at Sirta at 100 m a.g.l. every 3h and their altitude; Middle graphs illustrate the wind rose (radial axis in km/h); Right graphs represent the chemical  
3 composition, in  $\mu\text{g}/\text{m}^3$  of submicron particle (organic, nitrate, sulphate, ammonium, chloride and black carbon in green, blue, red, orange, pink and dark grey,  
4 respectively), the contribution of traffic and wood-burning to BC, the  $\text{BC}/\text{SO}_4^{2-}$  ratio, and temperature, RH and BLH